

MARTIN MARIETTA ENERGY SYSTEMS LIBRARIES

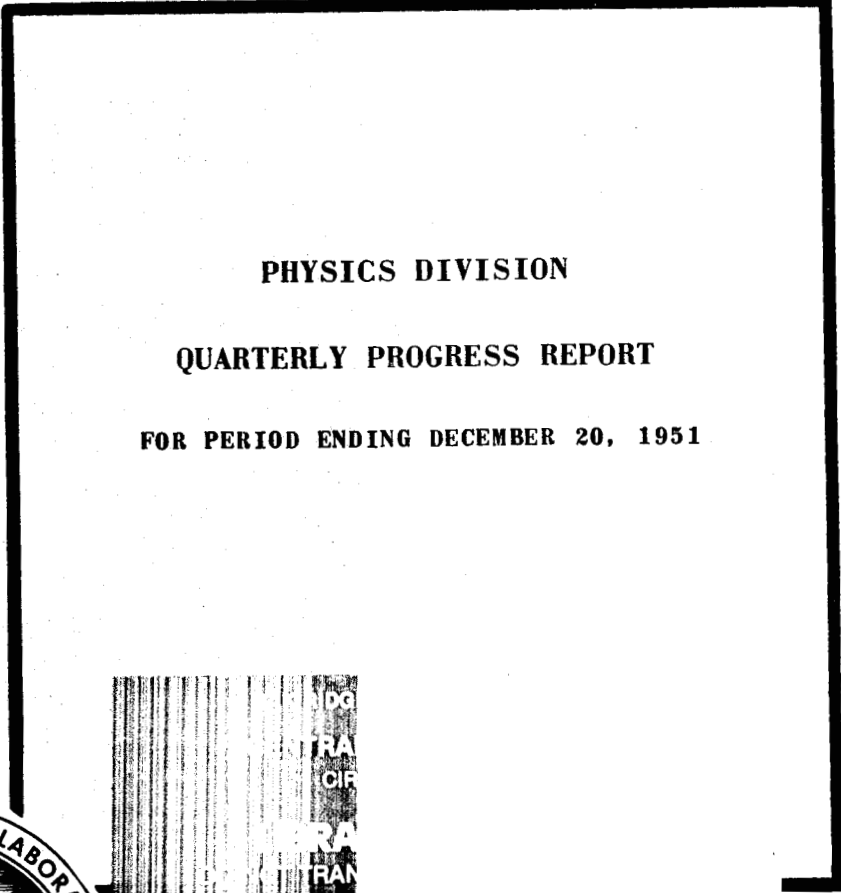


3 4456 0360942 3

TRAILLINE SCHOOL LIBRARY

ORNL-1278
Progress

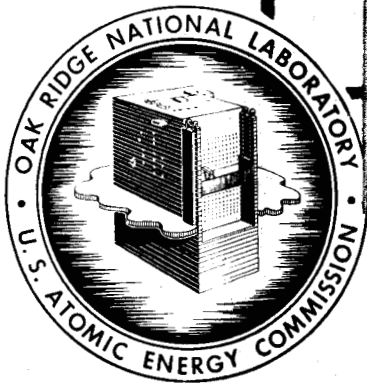
9a



PHYSICS DIVISION

QUARTERLY PROGRESS REPORT

FOR PERIOD ENDING DECEMBER 20, 1951



OAK RIDGE NATIONAL LABORATORY
OPERATED BY
CARBIDE AND CARBON CHEMICALS COMPANY
A DIVISION OF UNION CARBIDE AND CARBON CORPORATION



POST OFFICE BOX P
OAK RIDGE, TENNESSEE

ORNL-1278

This document consists of 50 pages.

Copy 9 of 331 copies. Series A.

Contract No. W-7405-eng-26

PHYSICS DIVISION
QUARTERLY PROGRESS REPORT
for Period Ending December 20, 1951

A. H. Snell, Director
E. O. Wollan, Associate Director

Edited by
W. M. Good

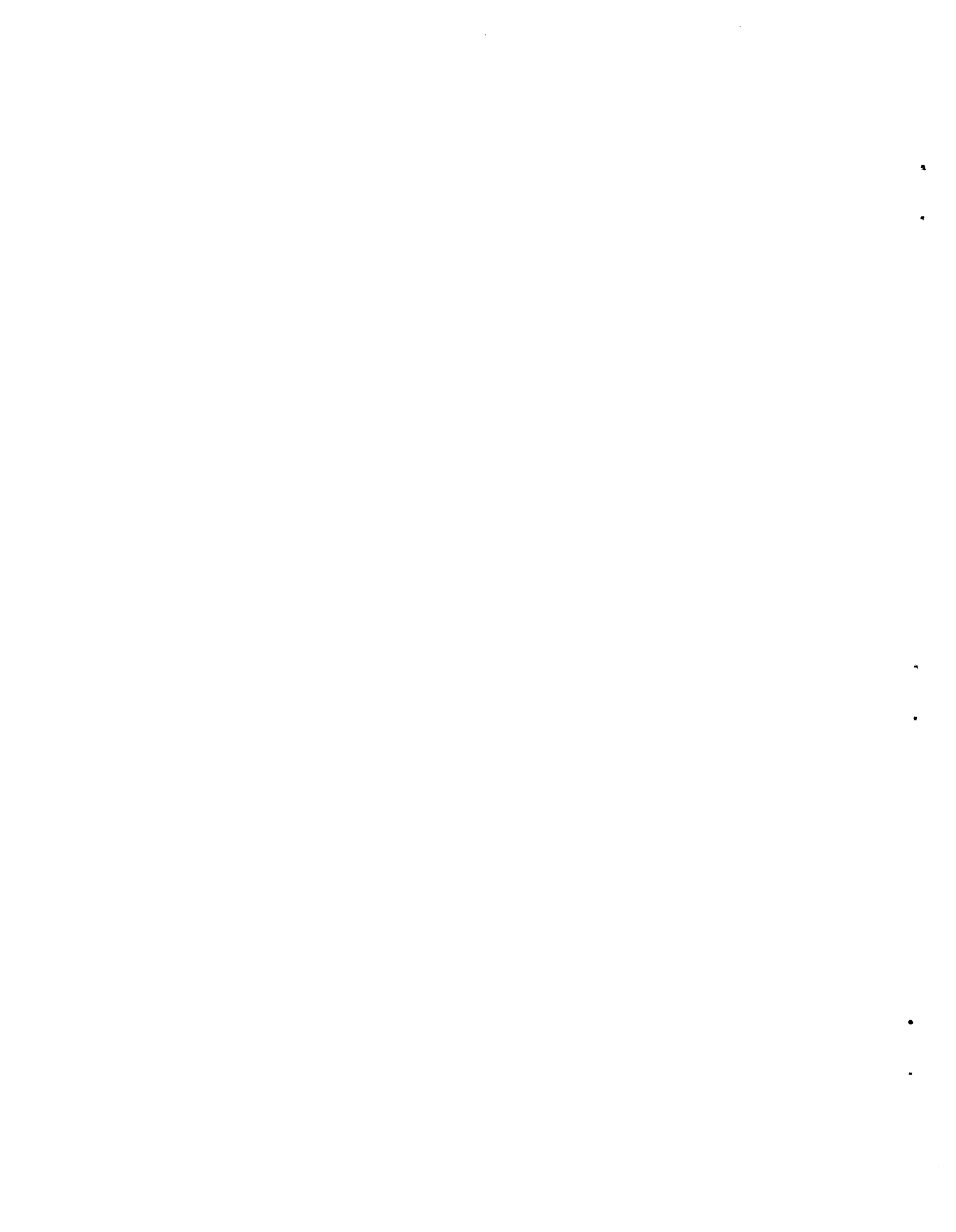
DATE ISSUED

ML 11 1952

OAK RIDGE NATIONAL LABORATORY
Operated by
CARBIDE AND CARBON CHEMICALS COMPANY
A Division of Union Carbide and Carbon Corporation
Post Office Box P
Oak Ridge, Tennessee



3 4456 0360942 3



INTERNAL DISTRIBUTION

- | | | | |
|--------|---|--------|----------------------|
| 1. | G. T. Felbeck (C&CCC) | 34. | L. D. Roberts |
| 2-3. | Chemistry Library | 35. | J. A. Lane |
| 4. | Physics Library | 36. | R. N. Lyon |
| 5. | Biology Library | 37. | W. C. Koehler |
| 6. | Health Physics Library | 38. | W. K. Ergen |
| 7. | Metallurgy Library | 39. | E. P. Blizard |
| 8-9. | Training School Library | 40. | M. E. Rose |
| 10. | Reactor Experimental
Engineering Library | 41. | G. E. Boyd |
| 11-14. | Central Files | 42. | Lewis Nelson |
| 15. | C. E. Center | 43. | R. W. Stoughton |
| 16. | C. E. Larson | 44. | C. E. Winters |
| 17. | W. B. Humes (K-25) | 45. | W. H. Jordan |
| 18. | L. B. Emlet (Y-12) | 46. | E. C. Campbell |
| 19. | A. M. Weinberg | 47. | D. S. Billington |
| 20. | E. H. Taylor | 48. | M. A. Bredig |
| 21. | E. D. Shipley | 49. | R. S. Livingston |
| 22. | E. J. Murphy | 50. | C. P. Keim |
| 23. | F. C. VonderLage | 51. | J. L. Meem |
| 24. | A. H. Snell | 52. | C. E. Clifford |
| 25. | J. A. Swartout | 53. | G. H. Clewett |
| 26. | A. Hollaender | 54. | C. D. Susano |
| 27. | K. Z. Morgan | 55. | C. J. Borkowski |
| 28. | F. L. Steahly | 56. | M. J. Skinner |
| 29. | M. T. Kelley | 57. | L. A. Rayburn |
| 30. | E. M. King | 58. | S. Bernstein |
| 31. | E. O. Wollan | 59. | P. M. Reyling |
| 32. | D. W. Cardwell | 60. | D. D. Cowen |
| 33. | A. S. Householder | 61-75. | Central Files (O.P.) |

EXTERNAL DISTRIBUTION

- 76-331. Given distribution as shown in TID 4500 under Physics Category.

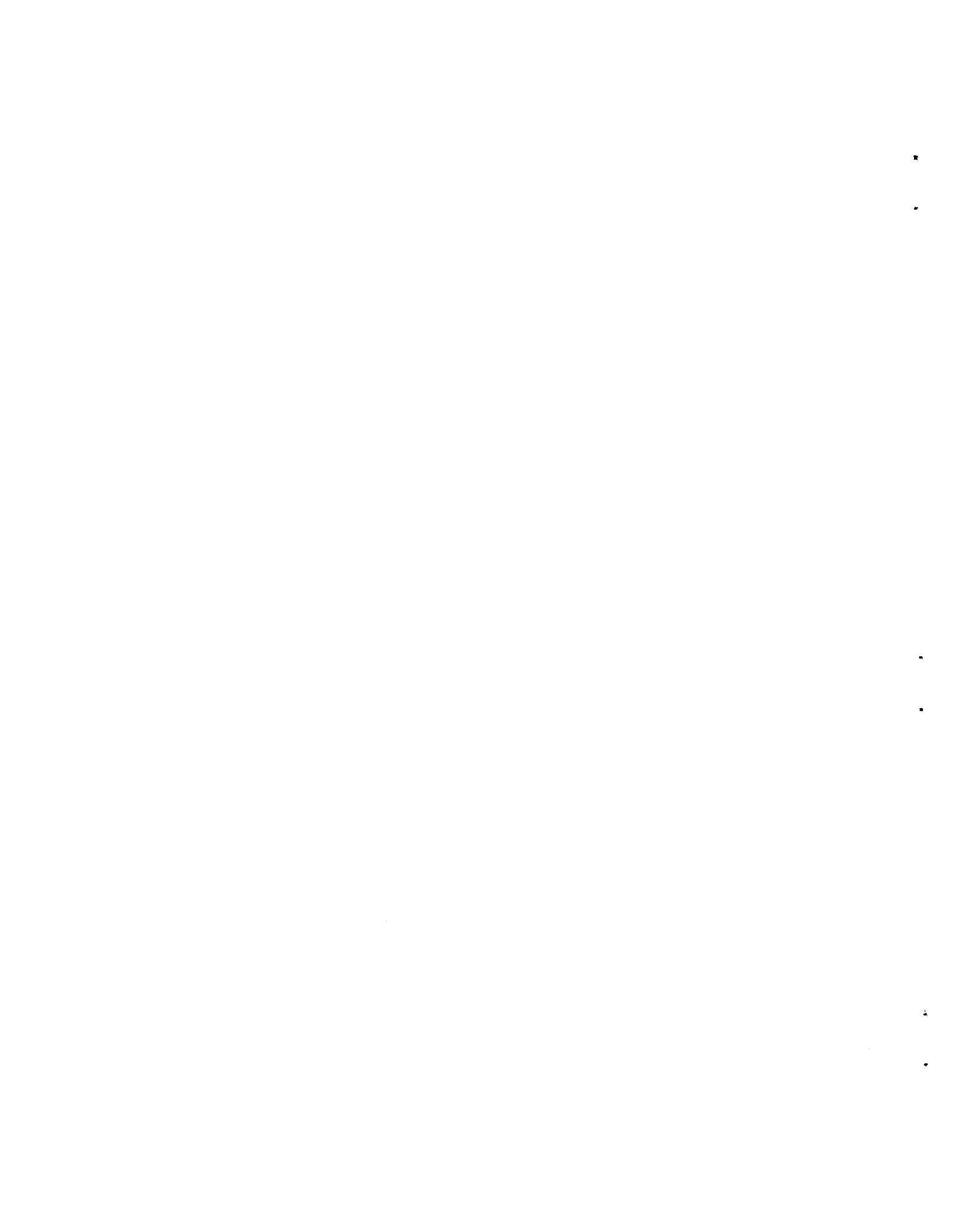
DISTRIBUTION PAGE TO BE REMOVED IF REPORT IS GIVEN PUBLIC DISTRIBUTION.

Physics Division quarterly progress reports previously issued in this series are as follows:

ORNL-325 supplement	December, January, and February, 1948-1949
ORNL-366	Period Ending June 15, 1949
ORNL-481	Period Ending September 25, 1949
ORNL-577	Period Ending December 15, 1949
ORNL-694	Period Ending March 15, 1950
ORNL-782	Period Ending June 15, 1950
ORNL-865	Period Ending September 20, 1950
ORNL-940	Period Ending December 20, 1950
ORNL-1005	Period Ending March 20, 1951
ORNL-1092	Period Ending June 20, 1951
ORNL-1164	Period Ending September 20, 1951

TABLE OF CONTENTS

	PAGE
PUBLICATIONS	xi
ANNOUNCEMENTS	xi
INTRODUCTION AND SUMMARY	1
1. HIGH-VOLTAGE PHYSICS	2
The $H^3(p,n)He^3$ Reaction	2
Total Neutron Cross-Section Measurements	3
Inelastic Scattering of Neutrons by Elemental Iron	4
(p,n) Threshold Determinations	5
The Reaction $Li^6(t,p)Li^8$	5
Cross Section vs. Energy of the Reaction $He^3(H^2,H^1)He^4$	8
2. RADIOACTIVITY AND NUCLEAR ISOMERISM	10
Internal Conversion in the Isomers Ta^{181} and Eu^{153}	10
Angular Correlation of Gamma Rays from Pd^{106}	11
3. NEUTRON DIFFRACTION	12
Neutron Scattering Studies of the Light Rare Earths	12
4. HEAVY-ION PHYSICS	17
Extrapolated Ionization Ranges of Ions Heavier than Protons	17
5. THEORETICAL PHYSICS	22
Angular Correlation of Nuclear Radiations	22
Triplet Neutron-Neutron Force	23
Angular Correlation of Radiations from Deuteron Stripping Reactions	24
Inner Bremsstrahlung Internal Conversions	24
A Rational One-Particle Relativistic Electron Theory	25
6. INSTRUMENTATION	27
Twenty-Channel Analyzer	27
Time-of-Flight Spectrometer	28
Servo for Curve Analyzer	29
Production and Detection of Heavy Ions	30
Optics of Polished Scintillation Phosphors	31
Adjustment of Voltage Distribution on the Electrodes of the 5819 Photomultiplier	33
Effect of a Longitudinal Magnetic Field on the Resolution of a 5819-NaI Scintillation Spectrometer	35
Neutron-Sensitive Phosphors	36
Neutron Response of NaI Scintillation Counters	38



LIST OF FIGURES

FIGURE	TITLE	PAGE
1.1	Differential Cross Section vs. Energy for the $H^3(p,n)He^3$ Reaction	2
1.2	Angular Distribution for the $H^3(p,n)He^3$ Reaction	3
1.3	Total Cross Section vs. Energy for the $H^3(p,n)He^3$ Reaction	3
1.4	Total Cross Section of Iron vs. Energy	4
1.5	Geometry for Inelastic Scattering Experiments	5
1.6	Yield of Gamma Rays vs. Energy of Neutrons on Iron	5
1.7	Activity vs. Time Following Bombardment of Li^6 with H^3	7
1.8	Cross Section vs. Energy for the $H^3(H^2,n)He^4$ Reaction	8
1.9	Cross Section vs. Energy for the $He^3(H^2,H^1)He^4$ Reaction	8
1.10	Yield of Protons from the Reaction $H^2(He^3,H^1)He^4$ with Incident He^3 Bombarding Energy	9
4.1	Differential Pumping System and Range Chamber	18
4.2	Ion-Chamber Current vs. Distance from Aperture, N^+ in Air	19
4.3	Range of N_2^+ in Air	19
4.4	Range of Ne^+ in Helium	19
4.5	Extrapolation of R_A vs. $1/P$ to Obtain R_E , for N_2^+ in Air	20
4.6	Range of Various Ions in Argon	20
4.7	Range of Various Ions in Nitrogen	21
4.8	Range of Various Ions in Helium	21
6.1	Gain of Type-6AG7 Tube as a Cathode Follower	28
6.2	Modification of Output Feedback Group of A-1 Amplifier	28
6.3	Servo for Curve Analyzer	29
6.4	Equipment for Ion Source and Electron Multiplier Response Studies	30
6.5	Reflection of a Ray of Light from the Cylindrical Surface of a Polished Phosphor	31

FIGURE	TITLE	PAGE
6.6	Reflection of Light from the Top Surface of a Polished Phosphor	32
6.7	Photocathode Emission Across the Cathode of Typical 5819 Photomultipliers	34
6.8	Resolution of Scintillation Spectrometer as a Function of Collector Voltage and First and Second Dynode Voltages	35
6.9	Pulse Spectrum Produced in LiI (SnI ₂ Activated) by Slow Neutrons	36
6.10	Pulse Spectrum Produced in LiI (SnI ₂ Activated) by Cs ¹³⁷ Gamma Rays	37

LIST OF TABLES

TABLE	TITLE	PAGE
1.1	(p, n) Threshold Determinations	6
2.1	Experimental and Theoretical Internal Conversion Coefficients	10
3.1	Factors for La_2O_3 Type Structures	14
3.2	Comparison of Calculated and Observed ($j F ^2/\sin\theta \sin 2\theta$)	15
3.3	Neutron Scattering Properties of Rare-Earth Nuclides	15
4.1	Effect of Pressure on the Observed Range, NTP (R_A)	21



PUBLICATIONS

A list of publications by the Physics Division during the past quarter follows:

"A Note on Isotropy in Nuclear Gamma-Radiation," G. B. Arfken, L. C. Biedenharn, and M. E. Rose, *Phys. Rev.* **84**, 89 (1951).

"Investigation of Nuclear Effects in Paramagnetic Single Crystals at Very Low Temperatures," S. F. Malaker, *Phys. Rev.* **84**, 133 (1951).

"Neutron Scattering and Polarization by Ferromagnetic Materials," C. G. Shull, E. O. Wollan, and W. C. Koehler, *Phys. Rev.* **84**, 912 (1951).

"Polarization and Alignment of Nuclei," A. Simon, M. E. Rose, and J. M. Jauch, *Phys. Rev.* **84**, 1155 (1951).

"Instrumentation and Control of Reactors," J. D. Trimmer and W. H. Jordan, *Nucleonics* **9**, No. 4, 60 (1951).

ANNOUNCEMENTS

During the period covered by this report W. J. Maynard and H. Reynolds joined the Physics Division staff.

For the year 1951 the following university staff members actively participated in the research of the Physics Division:

D. S. Hughes, University of Texas
J. Jauch, University of Iowa
T. M. Hahn, University of Kentucky
C. Sartain, University of Alabama
R. H. Rohrer, Emory University
W. E. Millet, University of Florida
D. B. Beard, Catholic University
H. C. Thomas, Mississippi State College

Three Cornell University undergraduates, J. Schwartz, F. Loeffler, and W. Harrison spent the summer with the Division. Three members, S. Podgor, R. Burnett, and J. Cassidy have terminated.

•

•

•

•

•

•

PHYSICS DIVISION QUARTERLY PROGRESS REPORT

INTRODUCTION AND SUMMARY

This report describes the progress made on the unclassified projects of the Physics Division for the period September 20 to December 20, 1951.

Neutron measurements made during this quarter included total neutron cross sections as well as a preliminary experiment on inelastic scattering. The energy range specifically reported is that from about 0.5 to about 3.6 Mev. These studies employed the 6-Mev Van de Graaff generator, and the nuclei studied for total cross sections and for inelastic scattering were isotopes of iron. Slow-neutron cross-section measurements are being made to show the initial performance of the time-of-flight spectrometer.

The problem of neutron detection is a continuing one; two items on the sensitivity of phosphors to neutrons are given. One of these deals with a phosphor for slow-neutron detection, the other deals with the response of NaI to fast neutrons.

In studies on radioactivity and nuclear isomerism, assignments of angular momentum and parity are reported for Ta^{181} , Eu^{153} , and Pd^{106} . In the cases of Ta^{181} and Eu^{153} the information comes from measurements of internal conversion where, as with Pd^{106} , the conclusion is drawn from angular correlations.

Lattice parameters and crystal structure for the oxides of some of the light rare earths have been established as a result of neutron diffraction studies. Simultaneously, these studies yield data from which the coherent cross sections are obtained. An analysis of these results is given.

Some reactions with light nuclei employing accelerated H^{3+} and He^{3+} are described. The tritium reaction

$Li^6(H^3, H^1)Li^8$, previously not described, has been identified, and a careful study has been made of the relative cross sections of the reactions $H^2(H^3, n)He^4$ and $H^2(He^3, H^1)He^4$. Results are discussed briefly in terms of a current theory of these reactions.

Some results have been achieved in the study of the stopping of heavy ions that have a few hundred kilovolts of energy. This report gives preliminary data on the ranges of a number of ions heavier than hydrogen in stopping media having the same range of masses.

Contributions to theory include a statement of the results obtained from a general approach to the problem of angular correlations. A note on the triplet neutron-neutron force states that considerations on this question show support in part of a previous conclusion that no strong like-particle triplet-state interactions occur. A study of the deuteron stripping process shows that a knowledge of the angular correlation of radiation following neutron stripping with the stripped particle can contribute to a determination of angular momenta of the states concerned.

Progress has been made on a number of instrumental problems. This report contains a description of the simplified twenty-channel pulse-height selector being studied. Work has started on a curve analyzer that will automatically separate the components of a spectra observed with a scintillation spectrometer. The analyzer also corrects for the statistics of the photomultiplier. Several contributions are made to scintillation counting and scintillation spectrometry. A brief description is given on the progress of heavy-ion production and detection.

PHYSICS DIVISION QUARTERLY PROGRESS REPORT

1. HIGH-VOLTAGE PHYSICS

THE $H^3(p,n)He^3$ REACTION

H. B. Willard J. K. Bair
J. D. Kington

The $H^3(p,n)He^3$ reaction is of interest theoretically because of the possibility of an excited state in He^4 and is of interest experimentally because of its convenience as a monoenergetic neutron source. The properties of this reaction were investigated previously⁽¹⁾ from threshold (1.019 Mev) to approximately

⁽¹⁾G. A. Jarvis, A. Hemmendinger, H. V. Argo, and R. F. Taschek, "Reaction Constants for $T^3(p,n)He^3$," *Phys. Rev.* **79**, 929 (1950).

2.8 Mev and have now been investigated to 5.0 Mev.

A thin (35-kev at threshold) zirconium tritide target⁽²⁾ on a tungsten backing was bombarded with a $1\text{-}\mu\text{a}$ beam of protons, and the neutrons produced were detected with a long counter. The yield in the forward direction is shown in Fig. 1.1; the absolute differential cross section was obtained by normalizing the data below 2.8 Mev to the Los Alamos curve.⁽¹⁾ The angular distribution of neutrons was then measured at laboratory angles of 0, 30, 60, 90,

⁽²⁾Loaned by T. W. Bonner, Rice Institute.

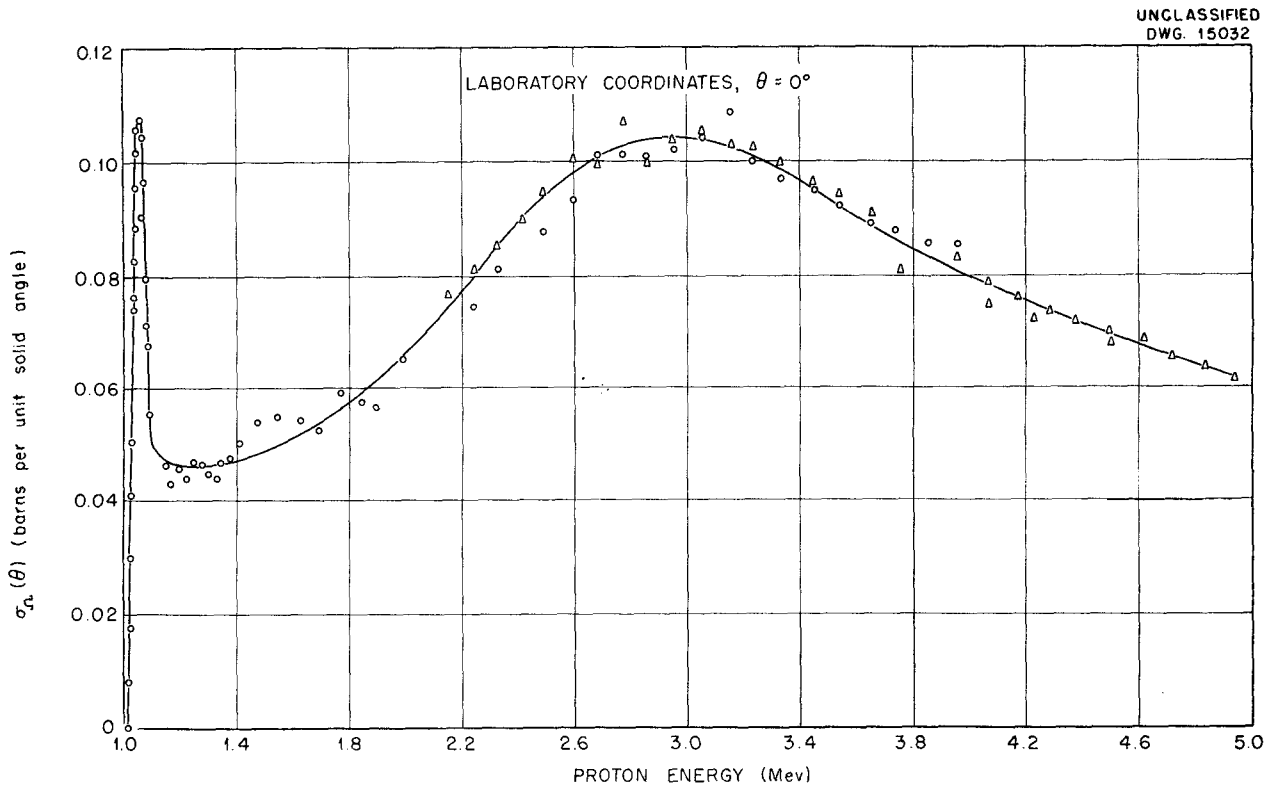


Fig. 1.1. Differential Cross Section vs. Energy for the $H^3(p,n)He^3$ Reaction.

and 120 deg. This data was transformed to the center-of-mass coordinate system and appears in Fig. 1.2. An analysis of the distribution into a series expansion in $\cos\phi$ was made and then integrated to give the total cross section as shown in Fig. 1.3. An attempt is being made to correlate the experimental results with theory.

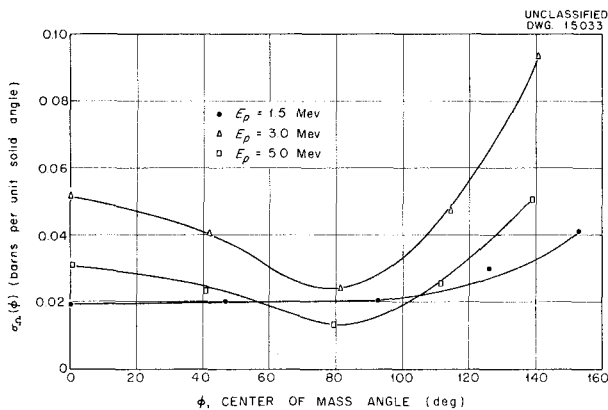


Fig. 1.2. Angular Distribution for the $H^3(p,n)He^3$ Reaction.

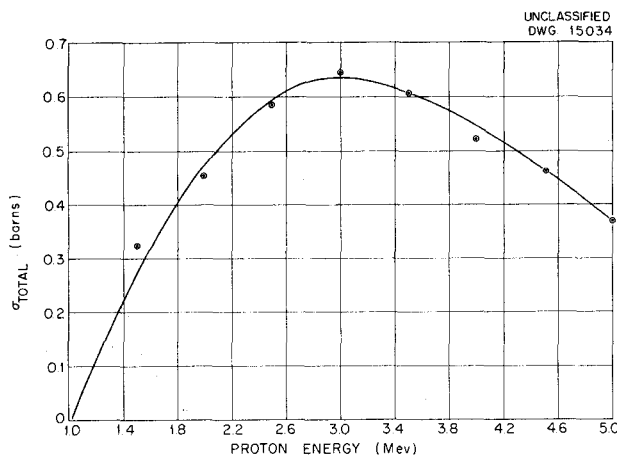


Fig. 1.3. Total Cross Section vs. Energy for the $H^3(p,n)He^3$ Reaction.

TOTAL NEUTRON CROSS-SECTION MEASUREMENTS

C. H. Johnson H. B. Willard
J. K. Bair

An apparatus for the measurement of total cross sections for fast neutrons was assembled and tested. Neutrons were produced by the $Li^7(p,n)Be^7$ reaction and detected with a propane recoil counter (sensitive volume, 1 in. in diameter, 4 in. in length, 1 atm of gas) located 8 in. from the target along the beam axis. Cylindrical scatterers 1 1/8 in. in diameter and of sufficient length to transmit 40 to 50% of the neutrons were interposed midway between the target and the detector for the measurements. Preliminary runs were made with carbon to check alignment and scattering from the sample holder. Background radiation was negligible. The secondary neutron group from $Li^7(p,n)Be^7$ was not detected by maintaining the bias at a sufficiently high level.

The total cross section of ordinary iron was then measured from 0.7 to 3.6 Mev with a resolution of 35 kev as shown in Fig. 1.4. Many unresolved resonances appear in the region of excitation. The data are in good agreement with that recently obtained at the University of Wisconsin by Miller.⁽³⁾

Plans are now under way to produce monoenergetic neutrons by the $H^3(p,n)He^3$ reaction (see previous section) with the use of a gas target. With this reaction as a source, the total cross sections for the light nuclei, as well as for heavy nuclei of interest, will

⁽³⁾D. Miller, to be published in *The Physical Review*.

PHYSICS DIVISION QUARTERLY PROGRESS REPORT

UNCLASSIFIED
DWG. 15035

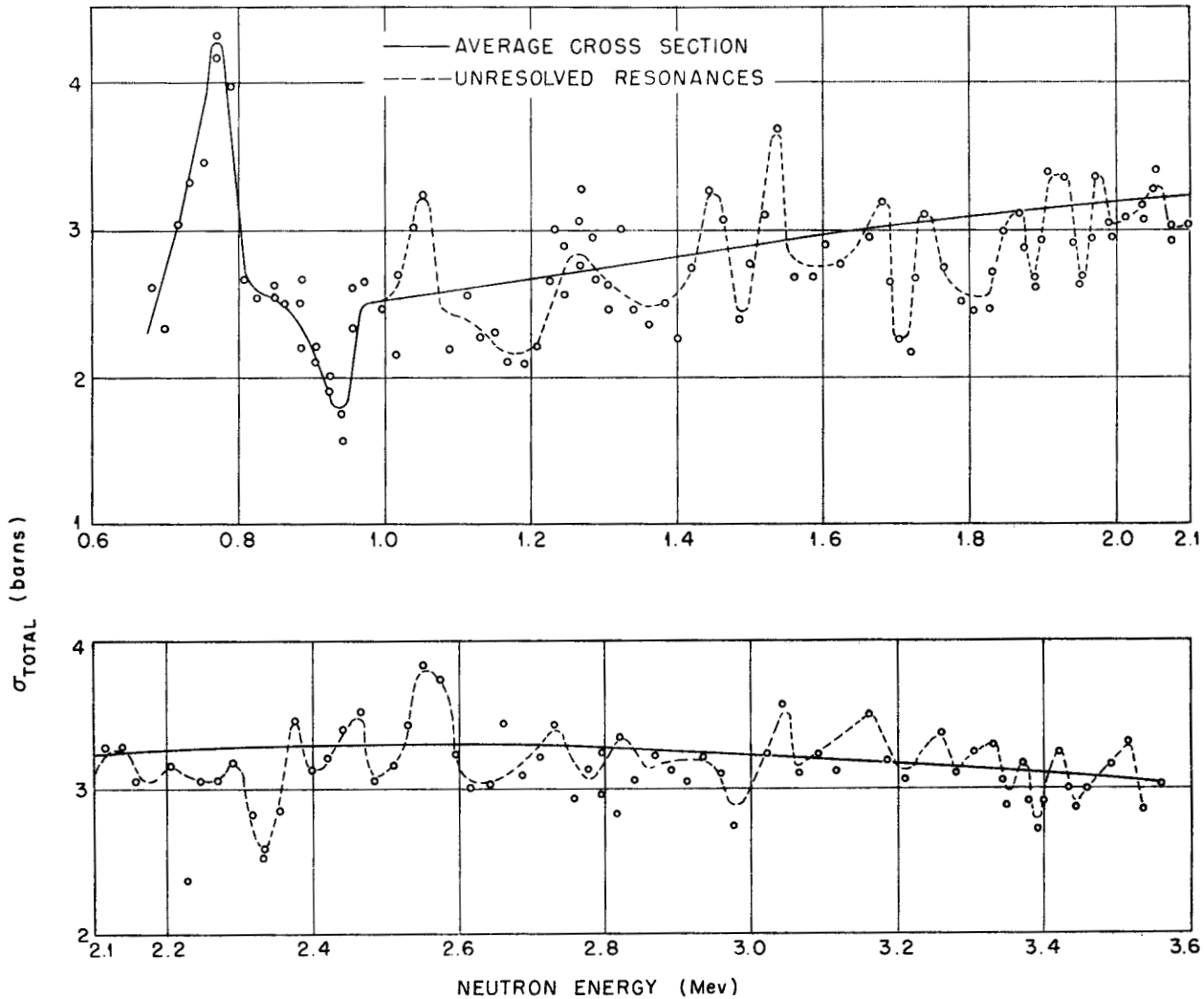


Fig. 1.4. Total Cross Section of Iron vs. Energy.

be extended with good resolution to 5 Mev (neutron energy). Neutrons will be detected by a high-pressure hydrogen recoil counter of greater sensitivity than that used in the present work.

INELASTIC SCATTERING OF NEUTRONS
BY ELEMENTAL IRON

J. K. Bair C. H. Johnson
H. B. Willard J. D. Kingston

A preliminary search for the first level excited by inelastic scattering

of fast neutrons in iron has been made. $Li^7(p,n)Be^7$ neutrons were scattered by a hollow cylinder of iron into a NaI crystal scintillation counter, and the response was measured as a function of incident neutron energy. The geometry of the setup, similar to that tried elsewhere,⁽⁴⁾ is illustrated in Fig. 1.5.

A rise in the counting rate was observed at a neutron bombarding

⁽⁴⁾H. B. Willard, W. M. Preston, and C. Goodman, *Nuclear Shielding Studies; IX. The Interaction of Fast Neutrons with Nuclei*, MIT Technical Report 45 (NP-1948) (Sept. 27, 1950).

energy of approximately 0.8 Mev when the integral pulse-height analyzer was set to count all pulses arising from gamma rays with energy greater than 0.5 Mev. This effect was accentuated by adjusting the differential pulse-height analyzer to count only those pulses corresponding to gamma-ray energies between 0.5 and 1.0 Mev as shown in Fig. 1.6. The background counting rate remained relatively constant when the iron cylinder was removed.

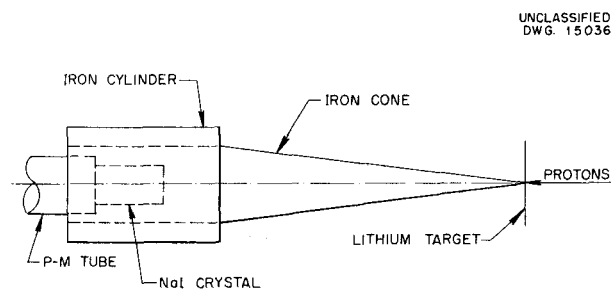


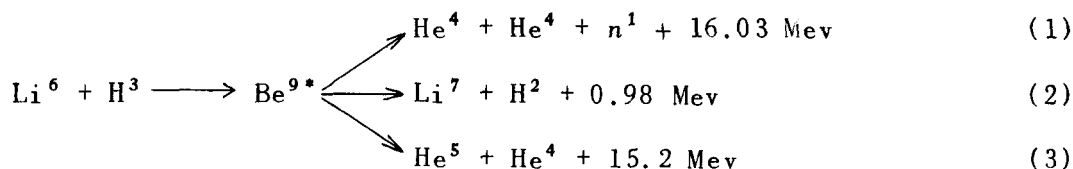
Fig. 1.5. Geometry for Inelastic Scattering Experiments.

It seems probable that this rise is due to inelastic scattering in Fe^{56} by the level at 0.822 Mev previously identified in beta-ray disintegration studies.⁽⁵⁾ This method will be tested further by application to lighter nuclei. Background radiation may be decreased by use of the $H^3(p,n)He^3$ reaction.

(p,n) THRESHOLD DETERMINATIONS

H. B. Willard J. K. Bair
J. D. Kington

The accurate determination of (p,n) thresholds will give information on the maximum disintegration energy available to the radioactive product



⁽⁵⁾A. C. G. Mitchell, "Spectroscopy of Some Artificially Radioactive Nuclei," *Revs. Modern Phys.* 22, 36, esp. p. 42 (1950).

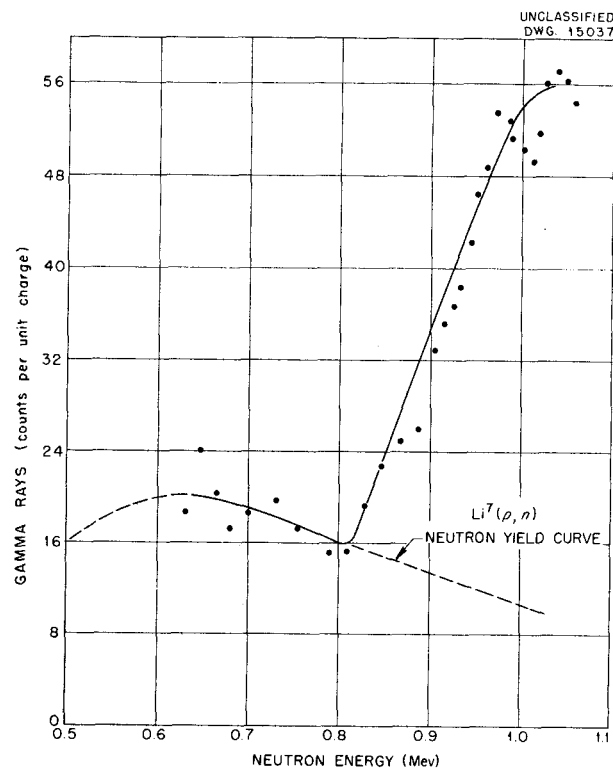


Fig. 1.6. Yield of Gamma Rays vs. Energy of Neutrons on Iron.

nucleus and the mass difference between product and target nuclei. A number of such thresholds have been measured by using readily available targets and by use of the Bonner-type counter as a neutron detector. The results are summarized in Table 1.1.

THE REACTION $Li^6(t,p)Li^8$

C. D. Moak W. M. Good
W. E. Kunz

The following reactions have been reported by Pepper *et al.*⁽⁶⁾ for Li^6 bombarded by tritons:

⁽⁶⁾T. P. Pepper, K. W. Allen, E. Almqvist, and J. T. Dewan, "Disintegration of Lithium by Tritons," *Phys. Rev.* 81, 315 (1951).

PHYSICS DIVISION QUARTERLY PROGRESS REPORT

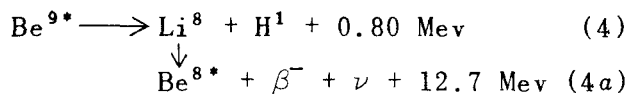
TABLE 1.1

(p,n) Threshold Determinations

TARGET NUCLEUS, X	PRODUCT NUCLEUS, Y	THRESHOLD, E_{th} (Mev)	$Q = \frac{-M_X}{M_X + 1} E_{th}$ (Mev)	$M_Y - M_X$ (amu*)	MAXIMUM DISINTEGRATION ENERGY OF Y FOR β^+ (Mev)
F ¹⁹	Ne ¹⁹	4.253 ± 0.005	-4.04	0.00350	2.24
Na ²³	Mg ²³	5.091 ± 0.010	-4.88	0.00440	3.08
Cu ⁶³	Zn ⁶³	4.200 ± 0.022	-4.13	0.00360	2.33
Cu ⁶⁵	Zn ⁶⁵	2.164 ± 0.015	-2.13	0.00145	0.33
Cb ⁹³	Mo ⁹³	2.683 ± 0.018	-2.65	0.00201	0.85
In ¹¹⁵	Sn ¹¹⁵	2.960 ± 0.019	-2.93	0.00231	1.13

*amu = atomic mass unit.

When Li⁷ is bombarded by deuterons there is observed not only these same modes of breakup of Be^{9*}, but also the mode



The Li⁶(t,p)Li⁸ reaction has been experimentally identified by observation of the beta rays in Eq. 4a and by the demonstration that the half life matches that of Li⁸; in addition, the beta rays were shown to have an energy end point greater than 10 Mev.

A triton beam of 5 μ a was accelerated to 350 kev in the Cockcroft-Walton apparatus and, after mass analysis, was passed between two electrostatic deflector plates to a thick Li₂SO₄ target mounted on a 5-mil aluminum window. Directly under the window was a NaI-5819 scintillation counter used to detect the beta rays. The electrostatic deflector plates were used to sweep the beam away from the vicinity of the target. A master timer controlled

the sequence of events for the half-life measurement so that after a 5-Mev bombardment from 0 to 3 sec, beta counts in 1/4-sec intervals could be obtained as a function of time. A plot of the count rate vs. delay after bombardment is shown in Fig. 1.7.

As a check on the energy of the beta rays, the scintillation counting equipment was biased so that pulses corresponding to a beta-ray energy of less than 10 Mev were rejected. With this bias setting a beta-ray counting rate five times background was still observed. Only three other beta emitters (B¹², 0.027 sec; N¹², 0.0125 sec; and N¹⁶, 7.2 sec) are known with energy end points above 10 Mev. The accuracy of the half-life determination is sufficient to rule these out as possible contaminations in the experiment.

Identification of the activity is thus accomplished by observing a combination of beta-ray energy and half life found only in Li⁸.

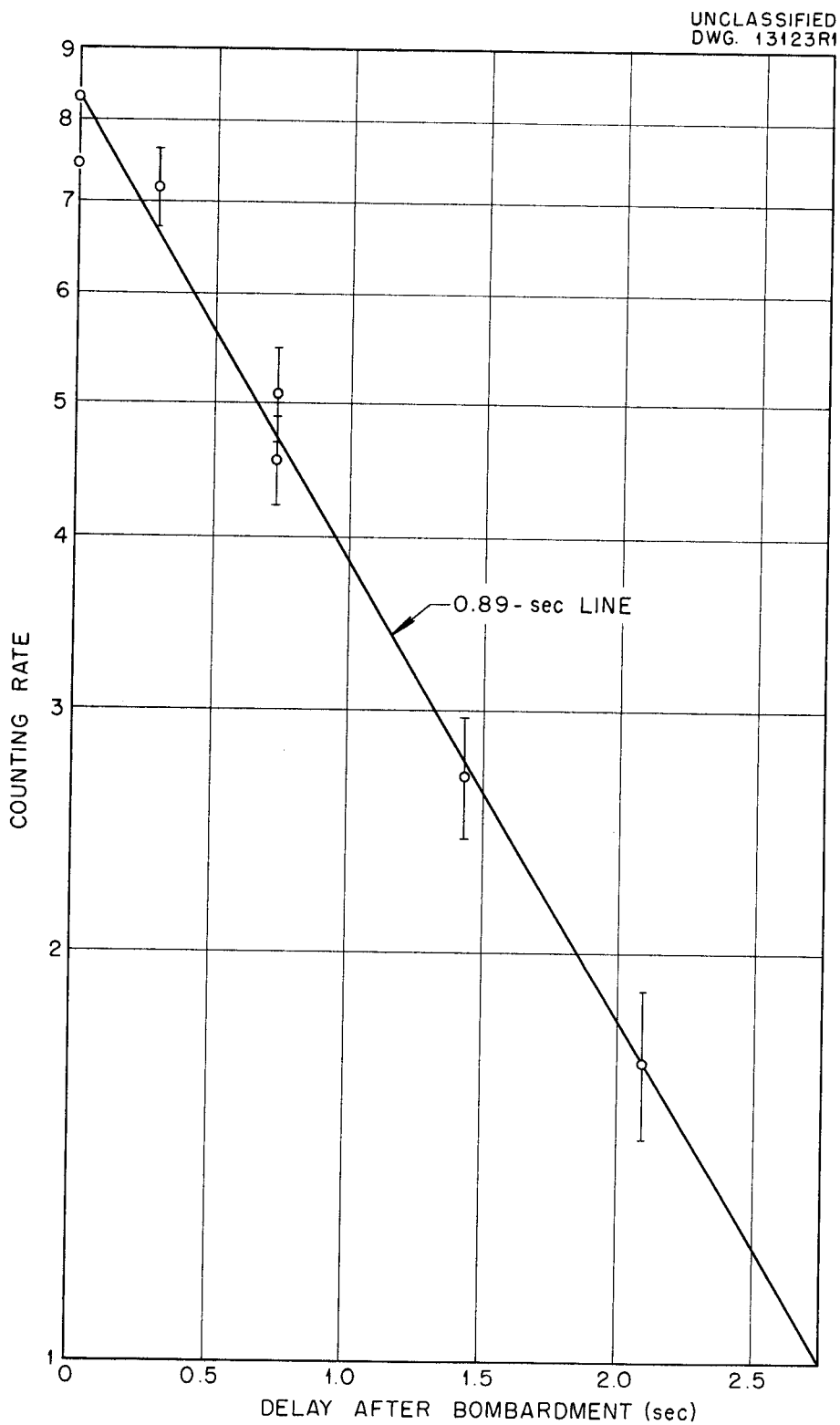


Fig. 1.7. Activity vs. Time Following Bombardment of Li^6 with H^3 .

PHYSICS DIVISION QUARTERLY PROGRESS REPORT

CROSS SECTION VS. ENERGY OF THE REACTION $\text{He}^3(\text{H}^2, \text{H}^1)\text{He}^4$

W. E. Kunz W. M. Good

Thin-target yield curves have been determined for the two following reactions:



The accelerated particles were He^{3+} and H^{3+} , and the same zirconium deuteride target was used for both reactions. The $\text{H}^3(\text{H}^2, n)\text{He}^4$ yield vs. energy was determined by counting the alpha particles per μa of beam with a proportional counter. In the same geometrical setup the number of alpha particles per μa of He^{3+} beam was obtained at 320 kev. The ratio of counts per μa from the $\text{He}^3(\text{H}^2, \text{H}^1)\text{He}^4$ reaction at 320 kev to the number of counts per μa from the $\text{H}^3(\text{H}^2, n)\text{He}^4$ reaction at any specified voltage equals the ratio of corresponding cross sections. A crystal counter was used to count the protons in the determination of the yield with energy from 80 to 400 kev of the $\text{He}^3(\text{H}^2, \text{H}^1)\text{He}^4$ reaction.

The average value for the peak of the $\text{H}^3(\text{H}^2, n)\text{He}^4$ reaction from absolute cross-section measurements by Bonner⁽⁷⁾ and by Allan and Poole⁽⁸⁾ is 5.87 barns. If the peak of the present yield curve is assumed to correspond to this average value, the cross section vs. energy curve of Fig. 1.8 is obtained. This normalization gives a cross-section curve for the reaction $\text{He}^3(\text{H}^2, \text{H}^1)\text{He}^4$ as given in Fig. 1.9. Both reactions give an isotropic angular distribution in the energy range in question as shown by published

⁽⁷⁾T. W. Bonner, *Cross Section for the Reaction $\text{T}(d, n)\text{He}^4$* , AECU-939 (Aug. 1950).

⁽⁸⁾D. L. Allan and M. J. Poole, "Experiments on the Reaction $\text{T}(d, n)^4\text{He}$," *Proc. Roy. Soc. (London)* **A204**, 488 (1951).

results on the $\text{H}^3(\text{H}^2, n)\text{He}^4$ reaction and results reported previously on the $\text{He}^3(\text{H}^2, \text{H}^1)\text{He}^4$ reaction.⁽⁹⁾

⁽⁹⁾W. M. Good, W. E. Kunz, and C. D. Moak, "Charged-Particle Reactions," *Physics Division Quarterly Progress Report for Period Ending September 20, 1951*, ORNL-1164.

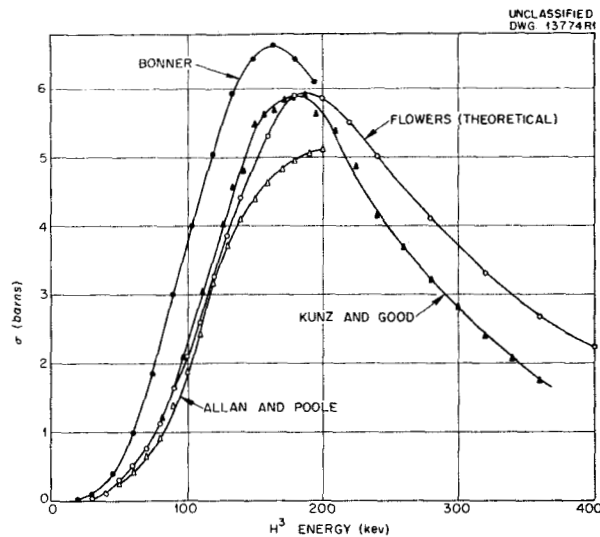


Fig. 1.8. Cross Section vs. Energy for the $\text{H}^3(\text{H}^2, n)\text{He}^4$ Reaction.

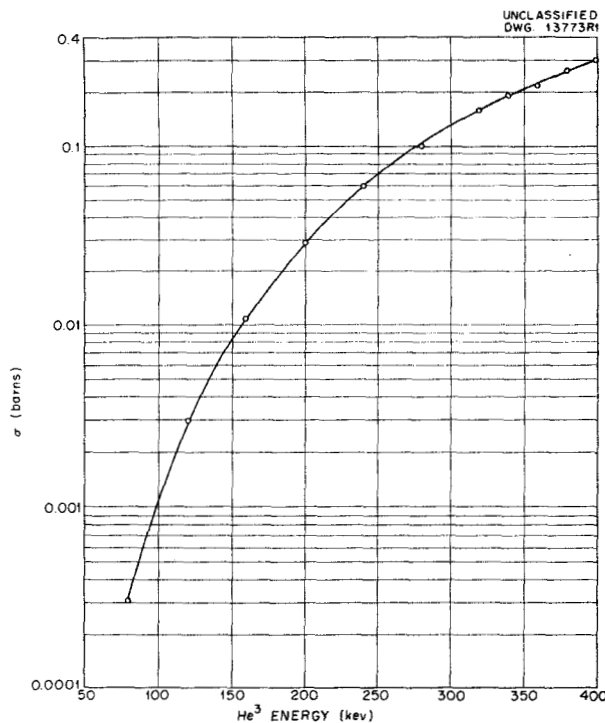


Fig. 1.9. Cross Section vs. Energy for the $\text{He}^3(\text{H}^2, \text{H}^1)\text{He}^4$ Reaction.

Figure 1.8 also shows a theoretical cross-section calculation by Flowers. This makes use of two nuclear parameters obtained from the experimental results and exact coulomb wave functions instead of the W.K.B. approximation for barrier penetration. Since the $\text{He}^3(\text{H}^2, \text{H}^1)\text{He}^4$ reaction is the mirror reaction of $\text{H}^3(\text{H}^2, n)\text{He}^4$ and the exci-

tation energies are approximately the same, a calculation of the $\text{He}^3(\text{H}^2, \text{H}^1)\text{He}^4$ cross section was made by this method by using the same nuclear parameters as were used in the $\text{H}^3(\text{H}^2, n)\text{He}^4$ calculation. From Fig. 1.10, it can be seen that the $\text{He}^3(\text{H}^2, \text{H}^1)\text{He}^4$ cross section differs markedly from the calculated results.

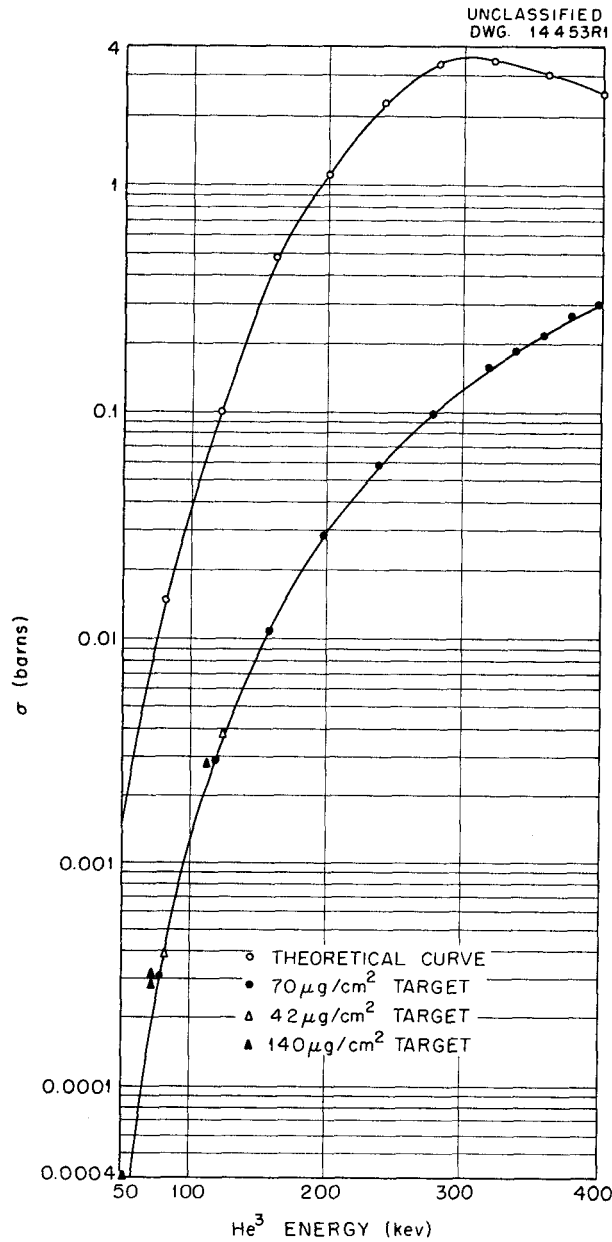


Fig. 1.10. Yield of Protons from the Reaction $\text{H}^2(\text{He}^3, \text{H}^1)\text{He}^4$ with Incident He^3 Bombarding Energy.

PHYSICS DIVISION QUARTERLY PROGRESS REPORT

2. RADIOACTIVITY AND NUCLEAR ISOMERISM

INTERNAL CONVERSION IN THE ISOMERS Ta¹⁸¹ AND Eu¹⁵³

F. K. McGowan

The 46-day Hf¹⁸¹ β⁻ activity is known to decay by a beta group to an excited state 612 keV above the ground state of Ta¹⁸¹.⁽¹⁾ The predominant decay of this excited state is by a gamma-ray cascade with energies of 132 and 480 keV. The initial state of the 132-keV transition, decaying with a $T_{1/2} = 22 \mu\text{sec}$, and the intermediate state at 480 keV above the ground, decaying with a $T_{1/2} = 10^{-8}$ sec, are metastable.

By measuring the spectrum of the K x rays and the gamma ray (132 keV) in coincidence with the 480-keV gamma ray of the cascade with a coincidence scintillation spectrometer employing NaI detectors, the K-shell internal conversion coefficient is obtained. The observed intensity ratio of the K x rays to the gamma ray must be corrected for fluorescent yield, escape-peak intensity, fraction of detected gamma ray appearing in the

full energy peak, and effective detection efficiency. The experimental and theoretical internal conversion coefficients⁽²⁾ are tabulated in Table 2.1. It is concluded that the 132-keV transition is of the E2 type. The observed $K/(L + M)$ ratio of 0.5 ± 0.1 also lends strong support to the assignment of electric character to the transition. It is of interest to note the extremely large spread for the transition probability of two E2 transitions of equal energy represented by the nuclei Ta^{181*} (2.2×10^{-5} sec) and Os^{186*} (8.0×10^{-10} sec). If this large spread is attributed to the square of the multipole-moment matrix elements contained in the usual theoretical transition probability estimates, then the ratio of the square of the matrix elements of Ta^{181*} to Os^{186*} is 4×10^{-5} .

Measurements of the K-shell internal conversion coefficients and the angular correlation of a successive gamma-quanta cascade of Eu¹⁵³ are in progress.

⁽¹⁾F. K. McGowan, *Short-Lived Isomeric States of Nuclei*, ORNL-952, p. 80 (Mar. 13, 1951).

⁽²⁾M. E. Rose, G. H. Goertzel, B. I. Spinrad, J. Harr, and P. Strong, "The Internal Conversion Coefficients. I: The K-Shell," *Phys. Rev.* **83**, 79 (1951).

TABLE 2.1

Experimental and Theoretical Internal Conversion Coefficients

NUCLEUS	E_γ (keV)	EXPERIMENTAL, α_{exp}^K	THEORETICAL		
			α_1^K	α_2^K	β_1^K
$_{73}\text{Ta}^{181}$	132	0.51 ± 0.05	0.15	0.495	1.94
$_{63}\text{Eu}^{153}$	70	3.8 ± 0.2	0.63	2.9	5.7
$\text{Sm}^{153} \xrightarrow{\beta^-} \text{Eu}^{153}$	102	1.1 ± 0.2	0.25	1.2	1.6
$\text{Gd}^{153} \xrightarrow{K} \text{Eu}^{153}$	102	0.7			

The beta decay of Sm^{153} leads to an excited state of Eu^{153} followed by two gamma rays in cascade with energies of 70 and 102 kev. The excited state at 172 kev above the ground state is metastable, decaying with $T_{1/2} = 3.0 \times 10^{-9}$ sec. Also, the K-capture decay of Gd^{153} presumably leads to the 102-kev state in Eu^{153} . The K-shell internal coefficients, measured with a coincidence scintillation spectrometer using NaI detectors, are tabulated in Table 2.1. The theoretical coefficients were obtained by an extrapolation procedure.⁽³⁾ The 70-kev isomeric transition appears to be of the E2 + M1 type with a quadrupole to dipole intensity ratio of 2.0.

The values of $\alpha_{\text{exp}}^{\text{K}}$ for the 102-kev transition using a Sm^{153} source were obtained by measuring the intensity ratio of the K x ray to the gamma ray in coincidence with the 70-kev gamma ray and the K x ray from internal conversion of the 70-kev transition. Good agreement was obtained between the two measurements. Similar measurements of the intensity ratio of the K x ray to the gamma ray in coincidence with the K x ray from the K-capture decay of Gd^{153} yields $\alpha_{\text{exp}}^{\text{K}} = 0.7$. This discrepancy is not understood. Also, the $K/(L + M)$ ratio, measured with an anthracene scintillation spectrometer, is 3.5 ± 1 with sources of Gd^{153} . This ratio would indicate that the transition is either E1 or E2 + M1. The measurements concerning the 102-kev transition must be considered as preliminary until the discrepancies are removed.

Preliminary measurements of the directional angular correlation of the 70- and 102-kev cascade appear to be isotropic to within $\pm 2\%$.

⁽³⁾F. K. McGowan, "Measurements of Some K-Shell Internal Conversion Coefficients," *Phys. Rev.* **85**, 151 (1952).

ANGULAR CORRELATION OF GAMMA RAYS FROM Pd^{106}

G. B. Arfken E. D. Klema
F. K. McGowan

Two NaI scintillation spectrometers similar to those mentioned in the previous progress report⁽⁴⁾ have been constructed and put into use with a similar coincidence circuit for the measurement of the directional angular correlation of successive gamma rays from excited states of Pd^{106} .

The angular resolution of this apparatus has been measured with the annihilation quanta from a Na^{22} source and found to be ± 10 deg. The resolving time of the coincidence circuit is 10^{-7} sec.

The angular correlation of the gamma rays in the main cascade of Pd^{106} was first measured by Brady and Deutsch.⁽⁵⁾ Their measured value of the ratio of the coincidence counting rates at 180 and 90 deg was 1.5. Their suggested spin assignments, 0-2-0, for the three energy levels involved predict a ratio of 2.0.

In the present work this angular correlation was measured at 10-deg intervals from 90 to 180 deg. This experiment, in which differential pulse-height analyzers for gamma-ray energy discrimination are used, gives a ratio of 1.86. The counting rate was of the order of 2 counts/sec, and the random rate was about 10% of this rate. The observed ratio was corrected for the effect of the 512-kev gamma ray and the radiation that entered the window of the other pulse-height

⁽⁴⁾F. K. McGowan and E. D. Klema, "Short-Lived Isomers and Directional Angular Correlation of Successive Gamma Rays," *Physics Division Quarterly Progress Report for Period Ending September 20, 1951*, ORNL-1164, p. 17.

⁽⁵⁾E. L. Brady and M. Deutsch, "Angular Correlation of Successive Gamma-Rays," *Phys. Rev.* **78**, 558 (1950).

PHYSICS DIVISION QUARTERLY PROGRESS REPORT

analyzer when it was set just above the photoelectron peak caused by the 624-keV gamma ray. This correction to the ratio amounted to about 1%.

The present experiment strongly supports the suggested spin assignments 0-2-0 by removing most of the discrepancy between theory and experiment. It is also of some interest because it has been suggested elsewhere that a possible explanation of the ratio obtained by Brady and Deutsch might be spin assignments 1-2-1, giving spin 1 to the ground state of an even-even nucleus.

A series of experiments was carried out to measure the angular correlation between the 512-keV gamma ray of the main cascade and all pulses corresponding to more than 200, 300, or 400 keV of energy dissipated in the

NaI detector. The observed ratios were all 1.5 or smaller and clearly showed the need for energy discrimination. This interference has not yet been positively identified.

The correlation between the gamma ray (1.05 MeV) from the third to the first excited state and the second gamma ray (512 keV) of the main cascade has also been measured. The data are inconsistent with the assignment of spin 0, 1, 3, or 4 to the highest (1.55 MeV) excited state for all possible mixtures⁽⁶⁾ of dipole and quadrupole radiation. The assignment of spin 2 and the assumption of strong dipole-quadrupole mixing gives results in agreement with the experiment.

⁽⁶⁾D. S. Ling, Jr. and D. L. Falkoff, "Interference Effects in Gamma-Gamma Angular Correlations," *Phys. Rev.* **76**, 1639 (1949).

3. NEUTRON DIFFRACTION

NEUTRON SCATTERING STUDIES OF THE LIGHT RARE EARTHS

W. C. Koehler E. O. Wollan

A survey of the light rare-earth elements and isotopes has been undertaken in order to obtain nuclear scattering data for nuclides in this low mass-number region and to investigate the magnetic scattering of neutrons by ions of the 4f series. Results are reported at this time on the nuclear scattering cross sections of some of these rare-earth nuclides. Crystal structure information that has resulted from the neutron diffraction studies of the oxides is also given.

Samples of the oxides of lanthanum, praseodymium, and neodymium, originally supplied by the Ames Laboratories, were used in the investigations of

the rare earths of normal isotopic constitution. Oxides of cerium, enriched in Ce^{140} and Ce^{142} , and of neodymium, enriched in Nd^{142} , Nd^{144} , and Nd^{146} , which were obtained from the ORNL Stable Isotopes Division, were also investigated.

The hexagonal La_2O_3 is the most convenient form of the rare-earth sesquioxides for neutron diffraction measurements. A structure for this compound was first proposed by Zachariasen.⁽¹⁾ The lattice constants for La_2O_3 are given as $a_1 = 3.945 \text{ \AA}$ and $a_3 = 6.151 \text{ \AA}$ ⁽²⁾ with one molecule per unit cell. Zachariasen, on the basis of x-ray powder data and Laue

⁽¹⁾W. Zachariasen, "Die Kristallstruktur der A-Modifikation von den Sesquioxiden der seltenen Erdmetalle (La_2O_3 , Ce_2O_3 , Pr_2O_3 , Nd_2O_3)," *Z. Physik. Chem.* **123**, 134 (1926).

⁽²⁾R. W. G. Wyckoff, *Crystal Structures*, Vol. I, Interscience, New York, 1948.

patterns, proposed the following atomic positions: 2 La in $\pm(1/3, 2/3, u)$, where $u = 0.25$, and 3 O in $(v, v, 0)$ $(\bar{v}, 0, 0)$ $(0, \bar{v}, 0)$, where $v = 0.25$. This arrangement of oxygen atoms was criticized by Pauling⁽³⁾ who placed the oxygens in $(0, 0, 0)$ and $\pm(1/3, 2/3, v)$, where $v = 0.63$.

To resolve the question of the oxygen parameters, neutron diffraction patterns of the hexagonal form of La_2O_3 , Pr_2O_3 , Nd_2O_3 , $\text{Nd}_2^{142}\text{O}_3$, $\text{Nd}_2^{144}\text{O}_3$, and $\text{Nd}_2^{146}\text{O}_3$ were obtained and analyzed. In general, the range of scattering cross sections of nuclei for neutrons is not nearly so wide as in the case of the corresponding x ray, and different isotopes of the same element frequently exhibit markedly different neutron scattering properties. Thus it was expected that the neutron data from such a series of samples could be treated to give the oxygen positions unambiguously.

Structure factors based on the two structures, expressed as a function of f_M (the metal scattering amplitude), were calculated on the assumption that the metal parameter is exactly 0.25, as indicated by Zachariasen's single crystal data⁽⁴⁾ and with the oxygen amplitude $f_O = 0.58 \times 10^{-12}$ cm. The values are listed in Table 3.1. The lines (001) and (111) are of special interest because they are independent of the metal amplitudes. The observed intensities of the (001) and (111) reflections in the diffraction patterns of all the samples were immeasurably small. Further, the relative intensities of (102) and (110) are reversed on the two models for certain values of the metal-scattering amplitudes. These qualitative considerations, together with the absolute

intensity data described in the following, favor the Pauling model.

An attempt to refine the oxygen parameter was made by using the Pauling model. The function $(j|F|^2/\sin\theta \sin 2\theta)$ was plotted as a function of f_M for values of v ranging from 0.63 to 0.67. The metal parameter was taken to be exactly 0.25, which is the value given by Zachariasen. Then three parameters, the oxygen parameter v , a single temperature correction factor, and the metal scattering amplitude, were determined. The isotopic neodymium series was especially interesting because one of the isotopes, Nd^{144} , has a scattering cross section less than that of oxygen. The best fit to the data was obtained for $v = 0.65$ and $\theta = 420$ deg for all samples within experimental error.

The observed and calculated values of $(j|F|^2/\sin\theta \sin 2\theta)$ for the isotopic neodymium series are compared in Table 3.2. The agreement appears to be satisfactory even though relatively small samples were available for study. In summary, these neutron diffraction data indicate that in the hexagonal La_2O_3 structure the oxygen centers are in $(0, 0, 0)$ and $\pm(1/3, 2/3, v)$, where $v = 0.65 \pm 0.01$.

The nuclear scattering data obtained in this study are given in Table 3.3 with the inclusion, for convenience, of normal cerium, the scattering amplitude of which has previously been reported.⁽⁵⁾ The coherent cross sections were measured from the powder diffraction patterns, and the total cross sections were determined by measuring the transmission at 0.07 ev and correcting for capture with the pile oscillator results obtained by Pomerance. In one case, Nd_2O_3 , transmission measurements have also been

(3) L. Pauling, "XXIV. The Crystal Structure of the A-Modification of the Rare Earth Sesquioxides," *Z. Krist.* **69**, 415 (1929).

(4) W. Zachariasen, "VI. Kurzere Originalmitteilungen und Notizen," *Z. Krist.* **70**, 187 (1929).

(5) C. G. Shull, E. O. Wollan, and W. C. Koehler, "Neutron Diffraction," *Physics Division Quarterly Progress Report for Period Ending March 20, 1951*, ORNL-1005, p. 13.

PHYSICS DIVISION QUARTERLY PROGRESS REPORT

TABLE 3.1

Factors for La_2O_3 Type Structures

INDEX	$j F ^2$	
	PAULING MODEL, $u = 0.25, v = 0.65$	ZACHARIASEN MODEL, $u = 0.25, v = 0.25$
001	0.02072	6.056
100	$6f_M^2$	$6f_M^2 - 6.96f_M + 2.018$
002	$8f_M^2 - 1.773f_M + 0.09822$	$8f_M^2 - 13.92f_M + 6.056$
101	$36f_M^2 - 33.79f_M + 18.11$	$36f_M^2 + 4.037$
102	$12f_M^2 + 18.23f_M + 17.87$	$12f_M^2 + 13.92f_M + 4.037$
003	5.664	6.056
110	$24f_M^2 + 41.76f_M + 18.17$	$24f_M^2 - 13.92f_M + 10.09$
111	0.1243	20.18
103	$36f_M^2 + 12.91f_M + 7.368$	$36f_M^2 + 4.037$
200	$6f_M^2$	$6f_M^2 + 6.96f_M + 2.018$
112	$48f_M^2 - 10.64f_M + 0.5893$	$48f_M^2 + 27.84f_M + 20.18$
201	$36f_M^2 - 33.79f_M + 18.11$	$36f_M^2 + 4.037$
004	$8f_M^2 - 2.868f_M + 0.2570$	$8f_M^2 + 13.92f_M + 6.056$

made at 1.44 ev. A brief discussion of the results for each nuclide follows.

Lanthanum. The total cross section of lanthanum obtained from transmission measurements at 0.07 ev was 14.3 barns. This value is uncorrected for crystal effects and there may be an error of the order of $\pm 5\%$. The total scattering cross section of 9.3 barns is obtained by using Pomerance's thermal-capture value of 8.8 barns⁽⁶⁾ and by assuming a $1/v$ capture law. This value is close to

the coherent scattering cross section of lanthanum of 8.7 barns, therefore the spin dependence of scattering from lanthanum is small. Furthermore, the magnitude of these cross sections is approximately what would be expected from hard sphere scattering. These results are in general agreement with those of Harris, Muehlhause, and Thomas.⁽⁷⁾

Both the observations reported here and those mentioned in the

⁽⁶⁾H. Pomerance, "Thermal Neutron Capture Cross Sections," *Phys. Rev.* 83, 641, (1951).

⁽⁷⁾S. P. Harris, C. O. Muehlhause, and G. E. Thomas, "Low Energy Neutron Resonance Scattering and Absorption," *Phys. Rev.* 79, 11 (1950).

FOR PERIOD ENDING DECEMBER 20, 1951

TABLE 3.2
Comparison of Calculated and Observed ($j|F|^2/\sin\theta \sin 2\theta$)

INDEX	$\text{Nd}_2^{142}\text{O}_3$		$\text{Nd}_2^{144}\text{O}_3$		$\text{Nd}_2^{146}\text{O}_3$		Nd_2O_3	
	OBS.	CALC.	OBS.	CALC.	OBS.	CALC.	OBS.	CALC.
001		1.4		1.4		1.4		1.4
100	76	73.6	14	9.8	116	94	66	65
002	259	273	184	186	347	334	283	250
101								
102	375	371	233	227	426	407	369	354
003	~35	44	~35	44	~35	44	~35	44
110	493	459	232	226	508	517	428	432
111		0.8		0.8		0.8		0.8
103	383	414	146	147	494	510	350	374
200								
112								
201								

TABLE 3.3
Neutron Scattering Properties of Rare-Earth Nuclides

NUCLIDE	f (10^{-12} cm)	σ_{coh} (barns)	σ_{total} (barns)
La^{139}	0.83 ± 0.02	8.7	9.3
Ce^{140}	0.47 ± 0.01	2.8	2.8
Ce^{142}	0.45 ± 0.02	2.6	2.6
Ce	0.46	2.7	2.7
Nd^{142}	0.77 ± 0.03	7.5	
Nd^{144}	0.28 ± 0.02	1.0	
Nd^{146}	0.87 ± 0.02	9.5	
Nd	0.72 ± 0.02	6.5	~16
Pr^{141}	0.44 ± 0.02	2.4	~4

PHYSICS DIVISION QUARTERLY PROGRESS REPORT

preceding reference are considerably lower than the results of the Columbia group quoted by Adair.⁽⁸⁾

Cerium. The two major isotopic constituents of cerium are Ce^{140} and Ce^{142} , which together account for 99.55% of the normal mixture. The scattering amplitudes of Ce^{140} and Ce^{142} were obtained from the diffraction patterns of the samples in the form of CeO_2 , which crystallizes with the CaF_2 structure. Both these nuclides are even-even isotopes so that no spin effects are expected. Total cross sections of highly enriched samples of these two nuclides, after correction for capture by using the isotopic capture cross sections calculated by Pomerance,⁽⁹⁾ lead to total scattering cross sections equal to the coherent scattering cross sections. Both isotopes have low cross sections compared with the expected potential scattering, and so does normal cerium. Thus there are indicated positive energy resonances in both the major isotopes of cerium. These results are in apparent contradiction to those of Hibdon and Muehlhouse⁽¹⁰⁾ who have found potential scattering cross sections of 5.77 and 4.80 barns by using cobalt and manganese detected neutrons, respectively, and who find that the scattering at both energies is 100% potential.

A coherent cross section for normal cerium of 2.2 barns was reported earlier from this laboratory.⁽⁵⁾ A calculation of the coherent cross section of normal cerium from the isotopic amplitudes gives a value of 2.70 barns. The normal cerium oxide

sample previously used was prepared from reagent-grade cerium nitrate that possessed a small amount of high-capture impurity, probably samarium, which might affect the accuracy of the normal cerium results.

Neodymium. Two samples of Nd_2O_3 have been studied. One of supposedly high purity was found by Pomerance to have a capture cross section at thermal (0.025 eV) of 100 barns. Transmission measurements on this sample at 0.07 and 1.44 eV agree approximately with measurements of Arnold and Sturm.⁽¹¹⁾ Another sample of Nd_2O_3 was found by Pomerance to have a thermal-capture cross section of 50 barns. A total scattering cross section of approximately 16 barns is obtained for both samples by using these values of the capture cross section and by assuming a $1/v$ dependence. The low coherent cross section of neodymium, 6.51 barns, compared with a total cross section of 16 barns arises primarily from isotope incoherence.

The cross sections listed for the separated isotopes of neodymium are strictly correct only for the sample studied and must be corrected for the isotopic analysis. It is apparent, however, in view of the total cross section of normal neodymium and of the high isotope purity of the samples (>95% in each case), that these values are approximately correct for the individual nuclides. The three cases studied are all examples of zero-spin nuclei. The small amplitude for Nd^{144} indicates the presence of a positive energy resonance. The two nuclei, Ce^{142} and Nd^{142} , whose scattering amplitudes are 0.45×10^{-12} and 0.77×10^{-12} cm, respectively, are

⁽⁸⁾R. K. Adair, "Neutron Cross Sections of the Elements," *Revs. Modern Phys.* 22, 249 (1950).

⁽⁹⁾H. Pomerance, private communication.

⁽¹⁰⁾C. T. Hibdon and C. O. Muehlhouse, "Neutron Cross Sections at 115 eV and 300 eV - I," *Phys. Rev.* 76, 100 (1949).

⁽¹¹⁾G. Arnold and W. J. Sturm, *The Total Neutron Cross-Section of Dysprosium and Neodymium*, MDDC-736 (Mar. 6, 1947).

the first pair of equal-mass-number zero-spin nuclei to be studied.

Praseodymium. The coherent and total scattering cross sections of praseodymium indicate a fairly strong spin dependence of scattering. Harris, Muehlhause, and Thomas⁽⁷⁾ suggest a resonance in praseodymium at 10 ev. The value that they give for the

thermal scattering cross section is greater than the values determined from the transmission measurements reported here by a factor of two, which would imply an even greater spin dependent scattering. Since there is evidence of a resonance, the procedure of correcting the intermediate energy transmission data by a $1/v$ capture law may not be valid.

4. HEAVY-ION PHYSICS

EXTRAPOLATED IONIZATION RANGES OF IONS HEAVIER THAN PROTONS

G. E. Evans P. M. Stier
C. F. Barnette V. L. DiRito

The extrapolated ionization ranges of the heavy ions H^+ , He^+ , N^+ , Ne^+ , N_2^+ , and A^+ have been measured in the gases He, N_2 , A, and air at energies from about 50 to 300 kev. For A^+ ions the maximum usable energy has been limited to about 160 kev by the size of the magnetic analyzer.

The apparatus is sketched in Fig. 4.1. A monoenergetic beam of heavy ions enters the range chamber by passing through three 0.030-in. pinholes. The gas in the range chamber, at a pressure of 0.1 to 10 mm Hg, is kept out of the accelerator proper by the differential pumping system. The ion chamber is mounted on a stainless steel rod supported by a Wilson seal. A synchronous motor drive permits varying at a constant rate the distance from the top of the range chamber to the top of the ion chamber. A system of micro-switch markers automatically place

1-in. fiduciary marks on the strip-chart record of ion-chamber current. The "entrance foil" of the ion chamber is a stainless steel screen that was heavily etched to improve its transparency. The chamber diameter is about 7.5 cm; its thickness is about 0.1 cm. The pressure in the range chamber is read on a McLeod gage and is monitored by an Alphatron gage. Each range determination was made at a series of pressures to determine the pressure-range relation as described in the text that follows. Since the ion chamber operates at the gas pressure of the range chamber, this implies that the ion-chamber characteristics vary from run to run at different pressures and in different gas atmospheres. For this reason, ion-chamber currents are reported in arbitrary but comparable relative units rather than as absolute specific ionization data. The use of such an arbitrary scale of ion-chamber current values does not affect the extrapolated ionization range determination. Experiments to determine absolute values of specific ionization are currently under way.

PHYSICS DIVISION QUARTERLY PROGRESS REPORT

UNCLASSIFIED
DWG. 14588

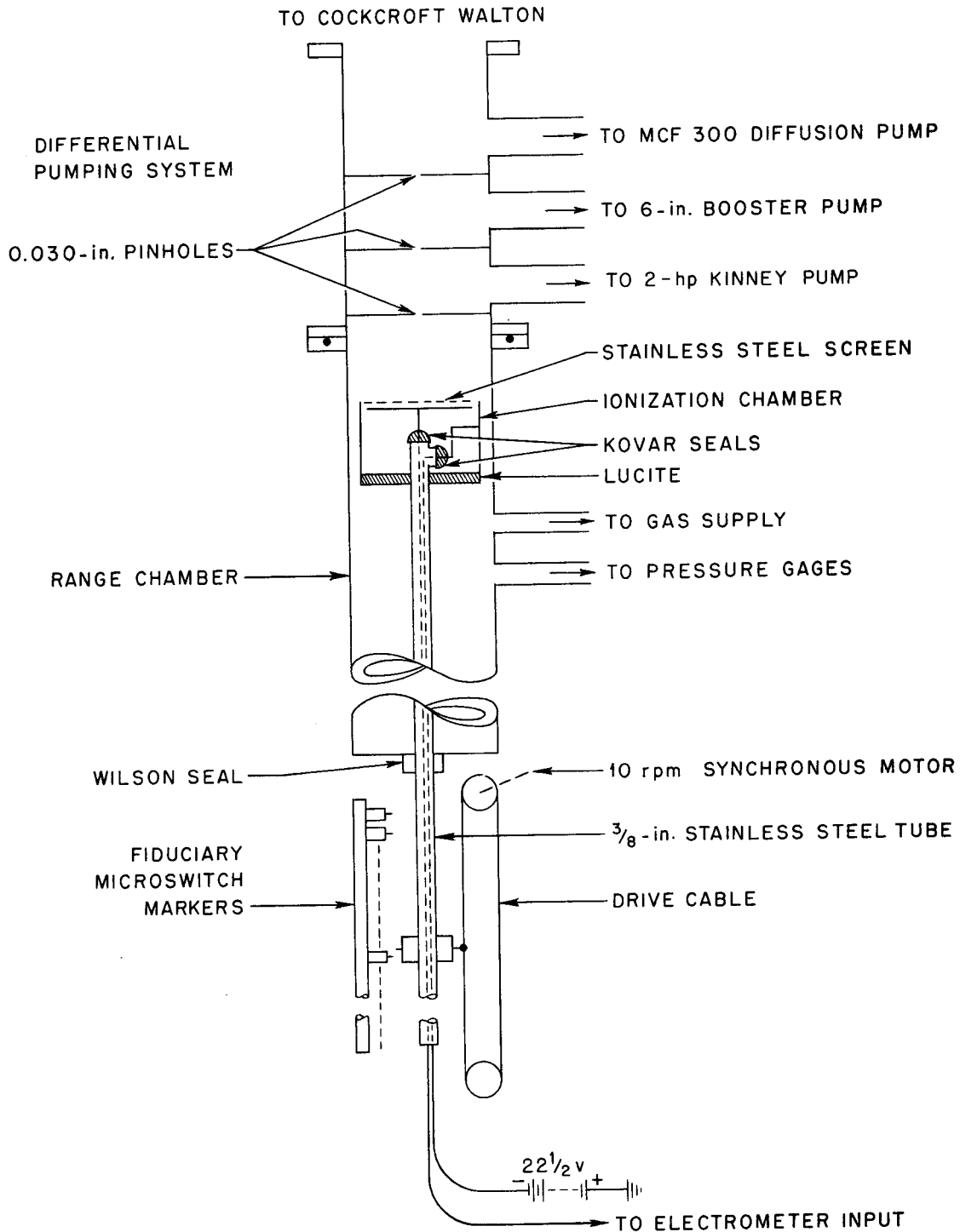


Fig. 4.1. Differential Pumping System and Range Chamber.

A typical ionization range curve as scaled from the strip-chart record is shown in Fig. 4.2. In practically all such curves for any of the heavy ions studied there exists a well-defined linear portion that can be extrapolated to intersect the zero current axis (point *D* in Fig. 4.2). In the following discussion the distance corresponding to *D* will be referred to as the "range at pressure *P*" (R_p); i.e., 10.46 in. is the range of N_2^+ in air at 0.692 mm Hg and 57 kev. These values of R_p are then multiplied by $25.4P/760$ to obtain the "observed range, NTP" (R_A) in millimeters,

$$R_A = \frac{25.4P}{760} R_p$$

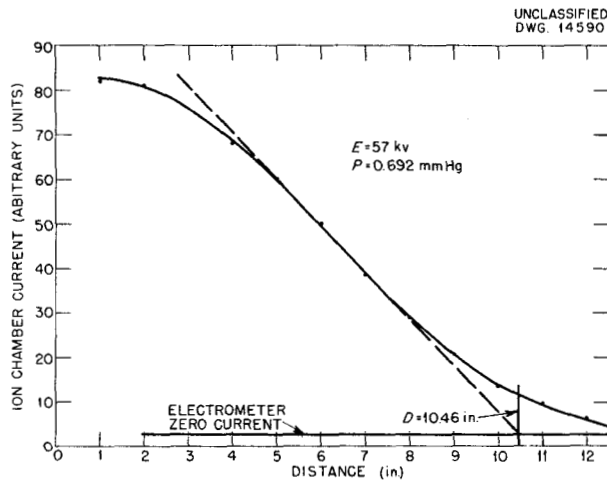


Fig. 4.2. Ion-Chamber Current vs. Distance from Aperture, N_2^+ in Air.

When these values of R_A are plotted against heavy-ion energy, a curve such as one of the curved lines in Fig. 4.3 is obtained. It will be noted that R_A decreases as the operating pressure decreases. The decrease in R_A seems to occur because at low pressures a significant portion of the total beam is scattered at angles so great that it escapes detection by the ion chamber and thus reduces the computed

value of R_A . If this explanation is correct, then the rate of change of R_A with P at a given energy should be greater for $M_1 = M_2$ than for $M_1 \gg M_2$ or $M_1 \ll M_2$, where M_1 and M_2 are the masses of the heavy ion and stopping gas atom, respectively. As illustrated in Fig. 4.4 for Ne^+ in helium, when $M_1 \gg M_2$ the values of R_A obtained at different pressures nearly fall on a single curve. Even here a slight but reproducible pressure dependence is evident. The extent to which R_A depends on P is indicated in Table 4.1, in qualitative agreement

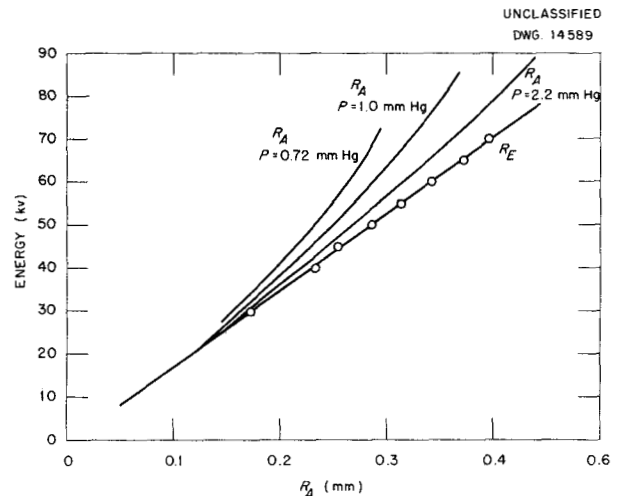


Fig. 4.3. Range of N_2^+ in Air.

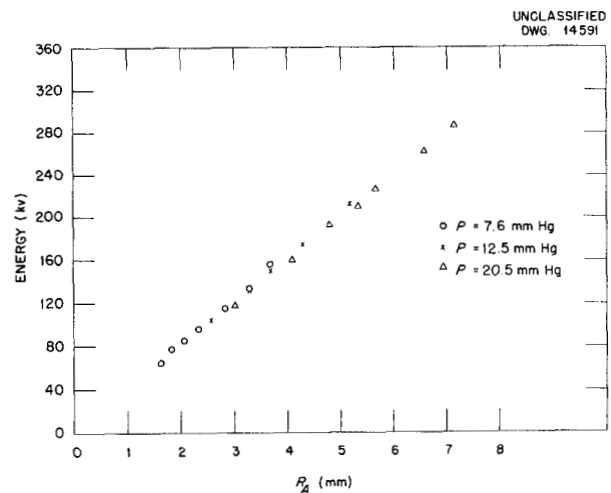


Fig. 4.4. Range of Ne^+ in Helium.

PHYSICS DIVISION QUARTERLY PROGRESS REPORT

with the order that would be predicted from the foregoing explanation.

Correction for Ion-Chamber Size. Since the value of R_A depends upon the pressure and also, as a consequence of the foregoing explanation, upon the ion-chamber size, it becomes important to obtain values of R_A that are independent of ion-chamber diameter and pressure of measurement. To

accomplish this, values of R_A have been plotted against $(1/P)$ and extrapolated to 1 atm pressure as shown in Fig. 4.5. The extrapolated values, R_E , should in principle be independent of ion-chamber size; this postulate will be verified experimentally as a further check of the theoretical explanation.

The plot of R_E vs. E shown with the actual extrapolated points on Fig. 4.3 is in nearly all cases a straight line. Values of R_E vs. E for various ions in argon are shown in Fig. 4.6, for various ions in N_2 in Fig. 4.7, and for various ions in helium in Fig. 4.8. Sufficient data are not yet available to determine the R_E vs. E curve for some heavy ion-stopping gas combinations; in these cases the R_A vs. E curve is shown for the highest pressure used.

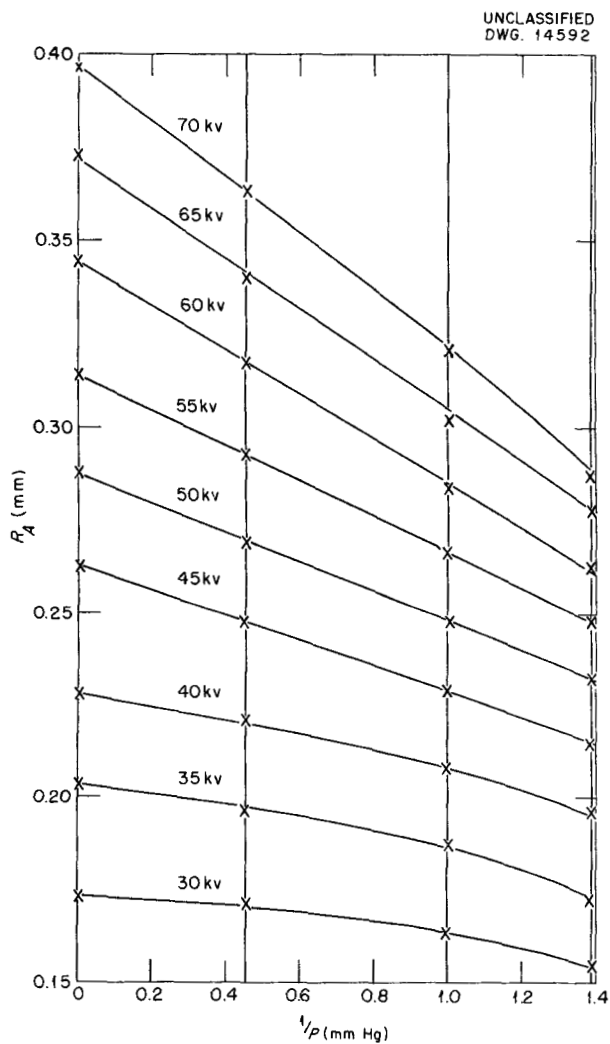


Fig. 4.5. Extrapolation of R_A vs. $1/P$ to Obtain R_E , for N_2^+ in Air.

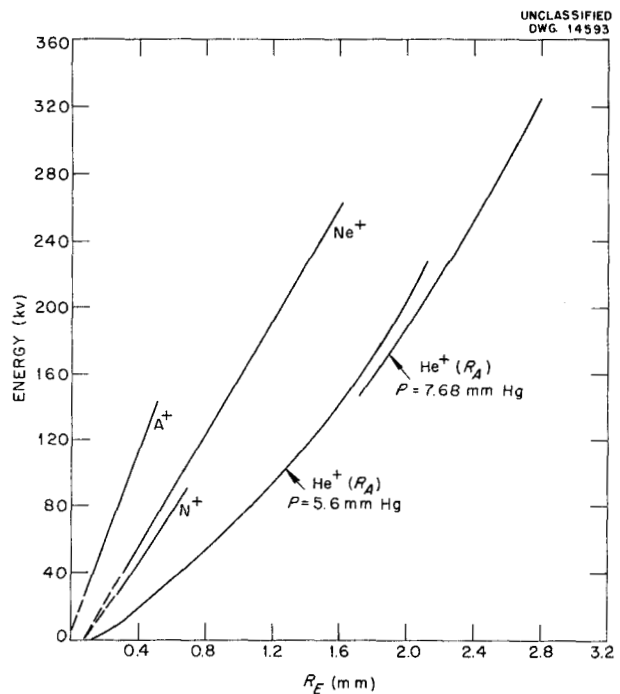


Fig. 4.6. Range of Various Ions in Argon.

TABLE 4.1

Effect of Pressure on the Observed Range, NTP (R_A)

HEAVY ION, M_1	STOPPING GAS, M_2	EFFECT OF P ON R_A
A^+	A	Extreme
N_2^+	N_2	Extreme
N_2^+	A	Extreme
A^+	N_2	Moderate to extreme
He^+	N_2	Moderate
N_2^+	He	Moderate
He^+	A	Extremely slight
Ne^+	He	Extremely slight
A^+	He	Extremely slight

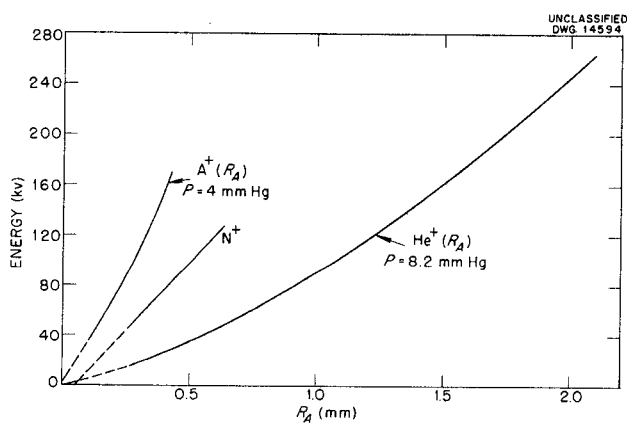


Fig. 4.7. Range of Various Ions in Nitrogen.

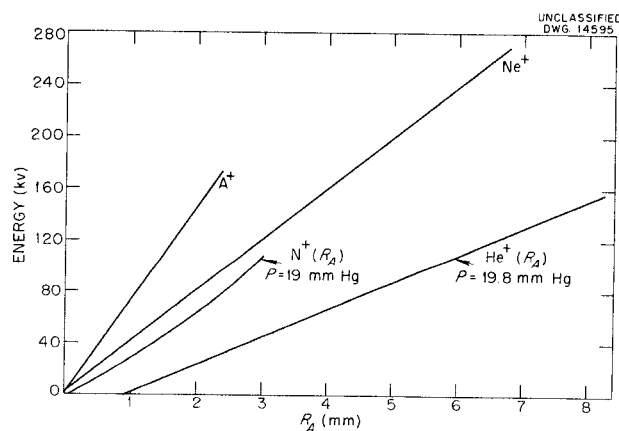


Fig. 4.8. Range of Various Ions in Helium.

PHYSICS DIVISION QUARTERLY PROGRESS REPORT

5. THEORETICAL PHYSICS

ANGULAR CORRELATION OF NUCLEAR RADIATIONS

M. E. Rose L. C. Biedenharn

The entire theory of angular correlation has been investigated. The principal purposes in this work are (1) to make the theory as practical as possible and reduce all calculational results to essentially numerical form where they can be readily used by experimentalists and (2) to obtain a better understanding of the underlying theory. Plans have been made to publish the results of this work as a survey article in the *Reviews of Modern Physics*.

The following questions have been studied:

1. The general theory for emission of two or more radiations including the case of nonsuccessive as well as successive emission. The radiations may be arbitrarily polarized and of an essentially arbitrary nature. From the general formulation the correlation function is obtained for particular radiations with a minimum of effort. Thus the tabulation of Racah coefficients (ORNL-1098) is of basic importance.
2. The general gamma-gamma correlation.
3. Correlations with alpha particles.
4. Effect of hyperfine structure and external magnetic field.

A number of new results have been obtained on the effect of hfs and external magnetic field. It is necessary to understand that when hfs is present the correlation tends to be obliterated in the sense that the

correlation function is more nearly isotropic than when no hfs is present. However, in many, if not most cases, the obliteration effect is not serious enough to hamper the experimental investigation of the correlation. The trouble occurring with hfs, and as it now appears hfs is usually present, is that the experiments cannot readily be interpreted, since an unknown parameter enters and the hfs splits with the nucleus in an excited (the intermediate) state. To avoid this difficulty an external magnetic field may be applied.

Three cases have been investigated:

1. Weak field (Larmor frequency \ll hfs frequency).
2. Strong field (Larmor frequency \gg hfs frequency).
3. Intermediate coupling (qualitatively, for electron momentum = $1/2$).

If the field is very strong and if one of the radiations is observed in the direction of the magnetic field, the effect of the hfs coupling is removed. A very strong field means that the magnetic energy of the electrons exceeds the hfs energy. This statement is true, however, only by virtue of the assumed parallelism of field and one of the propagation vectors. Otherwise a more drastic condition (nuclear magnetic energy \gg hfs energy) would have to apply. The first condition can be fulfilled in a large number of cases occurring in practice; the second cannot be fulfilled in any practical case. The error, which results because strict parallelism cannot be achieved, is of order θ , where θ is the half-angle of the cone defined by the detector in the magnetic field direction. When

the field is strong and one radiation is effectively parallel to the field, the condition to be observed is the one to be expected with no hfs and no field present.

In the use of magnetic fields to measure the g factor of nuclei in excited states it is necessary to have the following conditions fulfilled if it is desired to measure the sign of g :

1. The radiations and the field must not be coplanar.

2. The over-all efficiency of the detection arrangement must change when the radiation directions are interchanged. This could always be done with absorbers if the radiations have different energies.

TRIPLET NEUTRON-NEUTRON FORCE

F. G. Prohammer T. A. Welton

The calculation previously described on the triplet neutron-neutron force has been nearly completed. The experimental information that has been used is that no bound excited state of H^3 (or He^3) exists. In particular no bound 4S can exist, and the problem is to determine what restriction on the nuclear forces follows from this information. Assuming central forces (which seems plausible from several lines of argument), the wave equation contains a potential energy that involves the triplet neutron-proton force and the triplet neutron-neutron force (for H^3). Designating the protons by subscripts 2 and 3 and the neutron by subscript 1, the potential used is

$$V(r_{12}, r_{23}, r_{13}) = -Ae^{-2\epsilon r_{12}} - Ae^{-2\epsilon r_{13}} - Be^{-2\epsilon r_{23}},$$

where

$$A = 168.7 \text{ Mev,}$$

$$\epsilon = 6.945 \times 10^{12} \text{ cm}^{-1}.$$

The exponential fit to the triplet neutron-proton force is as reasonable a choice as is possible at this time. It fits the low-energy two-body information very well.

The neutron-neutron depth B is unknown, and the purpose of the calculation is to obtain information on its value. A variational expression for the energy of the 4S state has been obtained by using the 3-parameter trial function:

$$\psi = e^{-\frac{\epsilon}{2}[(a-c)r_{12} + (a+c)r_{13} + br_{23}]} - e^{-\frac{\epsilon}{2}[(a+c)r_{12} + (a-c)r_{13} + br_{23}]}$$

Such a trial function taken from the work of Rarita and Present, is known to give very good results for the 2S binding energy, a problem of similar complexity.

The procedure is to increase B until the energy becomes negative. This value then is an approximate upper limit for B . Thus far the binding energy has been calculated with B set equal to zero. The binding is probably then nonexistent; the lowest energy value to date is +12 Mev, and there is some indication that this is nearly the minimum.

It is fairly clear that any positive value of B comparable with A is absolutely excluded. Therefore, the triplet neutron-neutron interaction is repulsive, or weakly attractive. According to the conventional Majorana exchange hypothesis, the force should be *strongly* repulsive. It is now clear that no such repulsion is *required* to explain the lack of binding for the 4S state of the three-body problem.

PHYSICS DIVISION QUARTERLY PROGRESS REPORT

Although calculation on the present basis of the 4S phase shift for the slow n - d scattering is required to set a limiting negative value for B , this work makes a strong repulsion implausible.

The present result supports in part the result obtained by Christian and Noyes⁽¹⁾ from the medium energy (${}^1S + {}^3P + {}^1D$ phase shifts) proton-proton scattering. Their work indicates that no strong like-particle interaction occurs in a triplet state and thereby makes the exchange force untenable as the explanation for saturation.

ANGULAR CORRELATION OF RADIATIONS FROM DEUTERON STRIPPING REACTIONS⁽²⁾

L. C. Biedenharn K. Boyer⁽³⁾
R. A. Charpie

The angular distribution from deuteron stripping reactions⁽⁴⁾ has proved useful in determining the spin (J) and parity of nuclei formed in the reaction. When the orbital momentum transfer (l_n) is nonzero, however, J is not uniquely determined. If the nucleus emits subsequent radiation (for example, a gamma), this radiation should be correlated with the deuteron beam direction. In practice, measurements would be made of the coincidences of the gamma ray and the stripped protons of measured energy in order to identify the

⁽¹⁾R. S. Christian and H. P. Noyes, "The Proton-Proton Interaction," *Phys. Rev.* **79**, 85 (1950).

⁽²⁾A verbatim report of an abstract submitted at the 1952 New York meeting of *The American Physical Society*. A manuscript giving complete details is to be prepared at a later date for *The Physical Review*.

⁽³⁾Los Alamos Scientific Laboratory.

⁽⁴⁾S. T. Butler, "Angular Distributions from (d, p) and (d, n) Nuclear Reactions," *Proc. Roy. Soc. (London)* **A208**, 559 (1951).

emitting nuclear state.⁽⁵⁾ By observing this correlation further information on J might be obtained. The most informative case of this correlation is also the simplest, namely, where the target nucleus has zero spin ($j_i = 0$), since this eliminates the channel spin ambiguity and gives a restriction to a single l_n . For this case the rather simple answer is found that (by using Butler's assumptions⁽⁴⁾) the gamma is correlated with the direction of the (center of mass) recoil momentum, $K_d - K_p$, precisely as if the residual nucleus were formed by the resonance capture of the neutron from a plane wave directed along this axis; the angular distribution of the proton enters as a multiplicative factor only. The case $j_i \neq 0$ will be discussed at a later date.

INNER BREMSSTRAHLUNG INTERNAL CONVERSION

R. Osborne

Experimental evidence has recently been presented by Bruner⁽⁶⁾ for the existence of beta-decay processes in which the available nuclear energy is shared among three particles, the electron and the neutrino created in the process of nuclear decay and an orbital electron ejected from the atom as a consequence of the absorption of a gamma ray emitted by the newly created beta particle.

A theoretical investigation of this problem has been initiated. The point

⁽⁵⁾G. C. Phillips, N. P. Heydenberg, and D. B. Cowie, "Angular Correlation Studies of ($d; p, \gamma$) Processes of the Target Nuclei Li^6 , B^{10} , and O^{16} ," *Bull. Am. Phys. Soc.*, Abstract D7, p. 8 (Nov. 30, 1951). Isotropy was found in the cases observed, however.

⁽⁶⁾J. A. Bruner, "Experimental Evidence for Orbital Electron Emission Accompanying Beta-Decay," *Phys. Rev.* **84**, 282 (1951).

of view adopted for the purpose of this analysis consists essentially in a generalization of the usual inner bremsstrahlung calculation to the case in which the bremsstrahlung gamma ray ionizes the atom. The binding of the orbital electron is being neglected. It is anticipated that it will be feasible and possibly desirable to consider any or all of the various types of interactions between the nucleus and the electron-neutrino field usually assumed in the theory of beta decay.

A RATIONAL ONE-PARTICLE RELATIVISTIC ELECTRON THEORY

T. A. Welton

The various available formulations of quantum electrodynamics have been shown to be equivalent to hole theory in their predictions. The numerical results of this theory are good (not perfect) when the infinite mass and charge renormalizations are made to eliminate the divergences arising from electrodynamic and vacuum polarization effects, respectively. Although the rationale of the mass renormalization is clear cut, the same cannot be said of the charge renormalization, and the suspicion remains that the predictions of the hole theory are only partly and accidentally correct. In the following discussion an effort is made to formulate a rational one-particle theory, which will give correct answers for single-particle problems without introducing the machinery of pair production and vacuum polarization.

The Dirac equation is written in the following form:

$$\kappa\psi = K\psi, \quad (1)$$

where κ is the reciprocal Compton

wavelength of the electron and K is the operator;

$$\left. \begin{aligned} K &= K_0 + K_1 \\ K_0 &= i\gamma^\mu \frac{\partial}{\partial x^\mu} \\ K_1 &= \gamma^\mu \int dk [F_\mu(k)e^{i(kx)} \\ &\quad + \tilde{F}_\mu(k)e^{-i(kx)}] \end{aligned} \right\} (2)$$

The problem described by Eqs. 1 and 2 is that of the free particle coupled only to a radiation field, but a bound particle (hydrogen atom) can be treated by an obvious extension of the following procedure. The γ^μ 's are the usual Dirac matrices, and (kx) is a convenient notation for the four-dimensional scalar product $k_\mu x^\mu$. The quantities F_μ and \tilde{F}_μ are related to (but not identical with) the usual quantized amplitudes for the radiation field. They are matrices satisfying the invariant commutation rules:

$$\left. \begin{aligned} [F_\mu(k), F_{\mu'}(k')] & \\ &= [\tilde{F}_\mu(k)\tilde{F}_{\mu'}(k')] = 0 \\ [F_\mu(k), \tilde{F}_{\mu'}(k')] & \\ &= \frac{i\alpha}{4\pi^3} g_{\mu\mu'} \frac{\delta(k - k')}{(kk')}, \end{aligned} \right\} (3)$$

where α is the fine structure constant ("1/137"), $g_{\mu\mu'}$ is the usual covariant metric tensor, and $\delta(k - k')$ is the four-dimensional delta function that vanishes unless the four-vectors k and k' are equal, component by component.

The basic procedure is the calculation of corrections to an unperturbed wave function or to an unperturbed

PHYSICS DIVISION QUARTERLY PROGRESS REPORT

value of the electron mass. Note that such a procedure is relativistic in form (as well as in content) *ab initio*. In such a calculation, the quantities F_μ and \tilde{F}_μ are to be considered as

The simplest application is to the problem of the self-energy of a free electron. With the foregoing formalism, the correction to the mass of a free electron is

$$\Delta_K = \frac{i\alpha}{4\pi^3} \sum_i \int dk \frac{(\bar{\chi}_p \gamma^\mu \chi_{p-k}^s)(\bar{\chi}_{p-k}^s \gamma_\mu \chi_p)}{(kk)(K_p - K_{p-k}^s)}, \quad (5)$$

constant (but noncommuting) numbers until the desired mass correction or cross section has been obtained. This final expression is then averaged over the zero-point motion of the electromagnetic field according to the following rules:

$$\left. \begin{aligned} \overline{F_\mu(k)} &= \overline{\tilde{F}_\mu(k)} = \overline{F_\mu(k)F_{\mu'}(k')} \\ &= \overline{F_\mu(k)\tilde{F}_{\mu'}(k')} \\ &= \overline{\tilde{F}_\mu(k)F_{\mu'}(k')} = 0 \\ \overline{F_\mu(k)\tilde{F}_{\mu'}(k')} &= \frac{i\alpha}{4\pi^3} g_{\mu\mu'} \frac{\delta(k - k')}{(kk')} \end{aligned} \right\} (4)$$

with obvious extensions for products of more than two field quantities. No supplementary condition is used or needed since this is apparently a classical concept with no real place in a properly quantized theory.

where χ_p and χ_{p-k}^s are Dirac amplitudes for the unperturbed state (4-momentum = p) and a state with recoil 4-momentum k . The superscript s runs over two spin states and states with both signs of mass. The quantities K_p and K_{p-k}^s refer to the unperturbed mass and the mass in the intermediate state, respectively.

The 4-integral in Eq. 5 contains two poles that must be resolved by choosing a contour for the frequency integration that goes above the poles for negative frequency and below those for positive frequency. This rule is essentially that given by Feynman, and in fact Eq. 5 is identical in content with one given by him. Similar expressions can be obtained in more complicated situations, the most interesting is the mass correction for a bound electron, which is now being found. The expression differs from the conventional one in failing to give a vacuum polarization contribution.

6. INSTRUMENTATION

TWENTY-CHANNEL ANALYZER

G. G. Kelley P. R. Bell
 C. G. Goss

On the basis of experience gained through the use of the ten-channel analyzers described previously,⁽¹⁾ a twenty-channel analyzer was designed and constructed and has been in operation for several months. It differs from the ten-channel units in the layout of the pulse sorter and pulse-sorter power supply in that ten additional scalers and registers are required. Present ten-channel analyzers can be modified by replacing the pulse sorter and pulse-sorter power supply and adding an auxiliary unit containing ten scalers and registers. Alternatively, the present scaler panel and register board can be replaced by a slightly larger unit, as yet undesigned, containing the necessary extra equipment. The height of the pulse sorter and test pulse generator panels have been decreased to allow for this expansion.

The greatest source of dissatisfaction with the ten-channel analyzer has been associated with the need for gating the signal channel off during the analysis of a pulse; the amplifier may be resensitized during a succeeding pulse, which then will not be recorded in the proper channel. This need has been eliminated by an "inspector" circuit that permits a pulse to be analyzed only if a sufficient interval (2.3 μ sec) succeeding it is free from pulses. Another source of dissatisfaction has been the difficulty of keeping the reset operation fast

enough to prevent a pulse from being recorded in two adjacent channels if it falls near the boundary between them. The new analyzer interrogates all channels simultaneously and produces an output pulse in only one channel by the use of anti-coincidence circuitry between discriminators. An improved pulse-lengthener circuit drives the discriminators, which need not be particularly fast since they are not interrogated until at least 0.6 μ sec after the crest of an input signal. Each channel requires only one 12AT7 dual triode as a discriminator and half of another 12AT7 as a scaler driver tube. Mainly owing to the simplification in this part of the circuit, the new pulse-sorter chassis requires fewer tubes for twenty channels than the original analyzer required for ten channels. This simplification and a further refinement of design in the auxiliary circuitry make the new analyzer considerably more reliable than the old one. At present the stability is about equal to that of the old analyzer (1% channel width held for a 24-hr period), but from all indications poor quality tube sockets are responsible for most of the variation. A diagram of this unit and a description of the circuit will be published after it has been in use long enough to uncover whatever flaws may be present.

During the testing of the new pulse sorter, sources of error that had been previously overlooked were found external to this unit. An incremental gain variation of about 5% (see Fig. 6.1) was discovered in the output cathode follower of the A-1 amplifier. The modification shown in Fig. 6.2 has been made to correct this difficulty (see Fig. 1, MonP-323, for circuit diagram of A-1 amplifier). A type-5687 dual triode with both

⁽¹⁾G. G. Kelley, "A Multi-Channel Pulse Sorter," *Instrument Research and Development Quarterly Progress Report for Period Ending April 15, 1950*, ORNL-714, p. 29; G. G. Kelley, "Multi-Channel Analyzer," *Instrument Research and Development Quarterly Progress Report for Period Ending July 15, 1950*, ORNL-796, p. 63.

PHYSICS DIVISION QUARTERLY PROGRESS REPORT

halves in parallel replaces the cathode follower in the last feedback group and drives the load directly.

The motor driven 0.1% helipot in the test pulse generator has been another source of difficulty. It

has been found to cause an error of as much as 3% in window width when 40 dial divisions cover one channel.

TIME-OF-FLIGHT SPECTROMETER

G. S. Pawlicki⁽²⁾ E. C. Smith

The slow-neutron time-of-flight spectrometer is essentially completed. The rotating shutter has been successfully operated at 4800 rpm and the anticipated maximum speed is 6000 rpm. These speeds correspond to resolutions of 1.3 and 1.1 μsec per meter, respectively. The mechanical components of the spectrometer operate according to expectations.

As predicted by preliminary trials of the electronic equipment prior to delivery by the Instrument Department,

⁽²⁾ORINS research participant.

UNCLASSIFIED
DWG. 15039

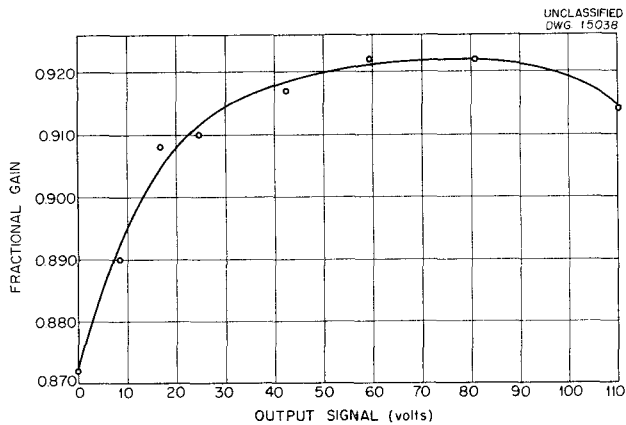


Fig. 6.1. Gain of Type-6AG7 Tube as a Cathode Follower.

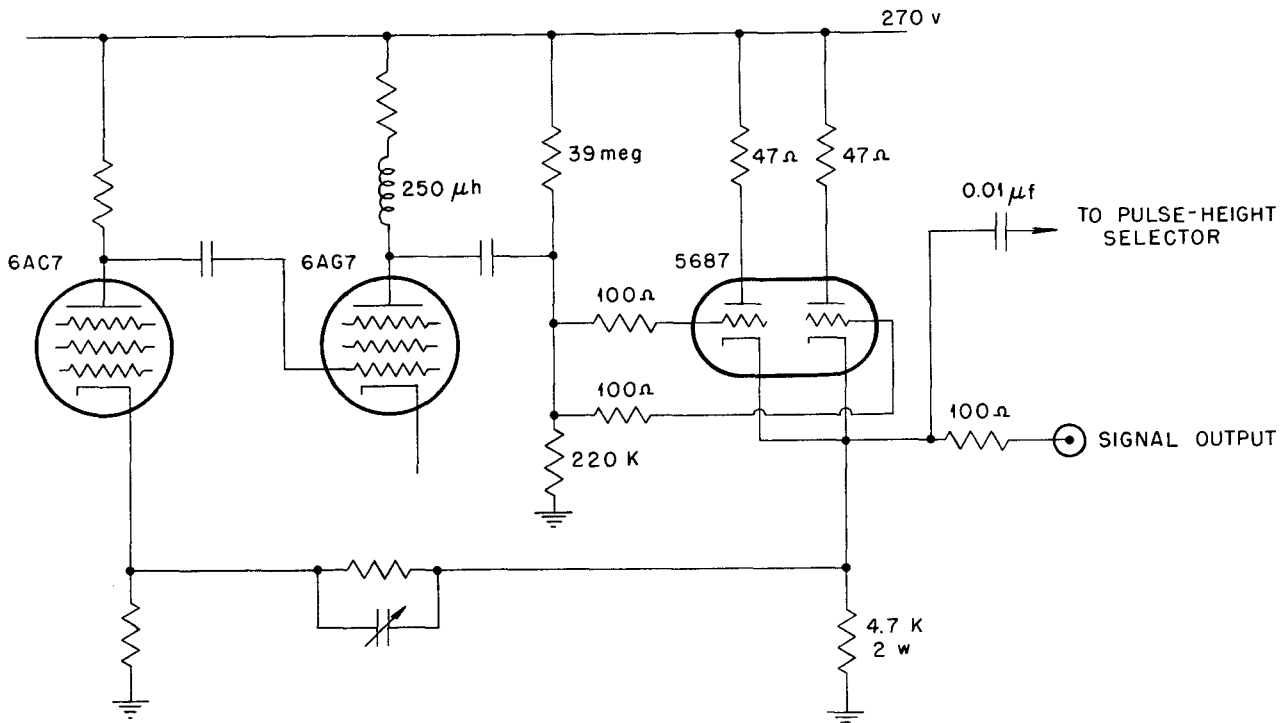


Fig. 6.2. Modification of Output Feedback Group of A-1 Amplifier.

all failures of the 84-channel counting equipment have been caused by tube failure. This is to be expected in a circuit involving 960 vacuum tubes.

Present operating time of the instrument is being devoted to preliminary spectrum and background measurements, to the spotting of known resonances, and to the determination of the operating characteristics of the instrument.

SERVO FOR CURVE ANALYZER

J. E. Francis P. R. Bell
S. H. Hanauer

A small-velocity servo that will balance the setting of one helipot against another to less than one division has been developed for use in a curve analyzer now under construction. The curve analyzer will analyze spectra from a scintillation spectrometer into the individual components by subtracting one component at a time. It will also

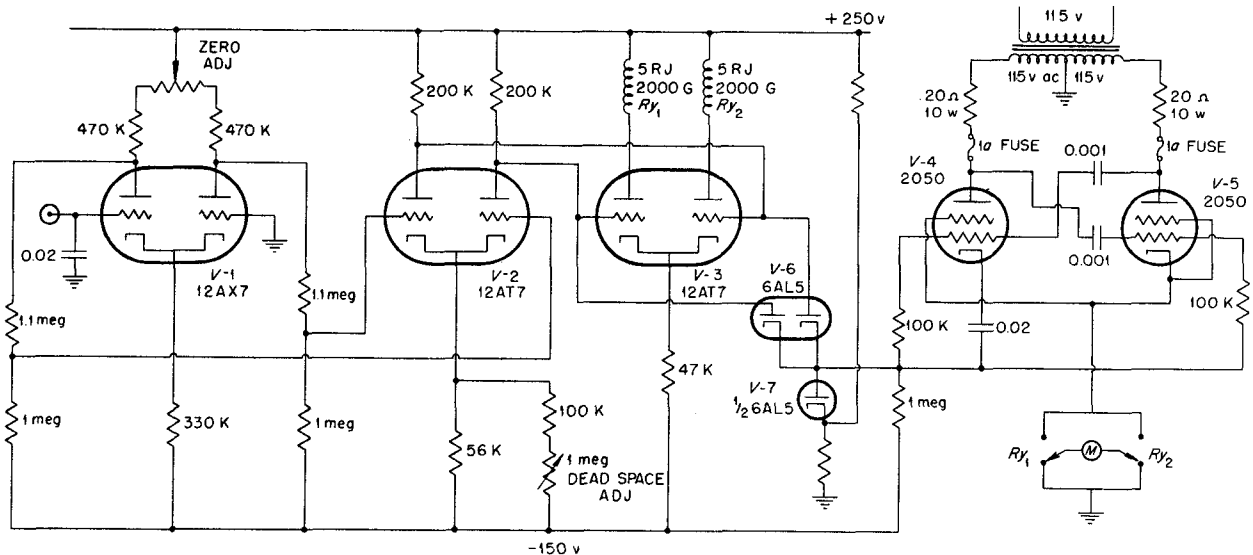
partly correct the shape of the curves for statistical spread introduced by the photomultiplier.

A circuit diagram of the servo is shown in Fig. 6.3. Any change in the potential of the ungrounded grid of V-1 causes an unbalance in the potential at the plates of V-1, and this in turn causes an unbalance of the plates of V-2. The unbalance of the plates at V-2 has two effects:

1. It causes a current to flow into one-half of V-3. This closes either relay No. 1 or No. 2, depending on the sign of the input signal to the servo. The closing of a relay connects a d-c motor in the cathode circuit of the 2050 thyratrons (V-4, V-5), and the direction of rotation of the motor is determined by the closed relay.

2. It raises the potential of one of the plates of the 6AL5 (V-6). This raises the d-c level of the grids of V-4 and V-5 so that they fire over a

UNCLASSIFIED
DWG. 15040



ALL RESISTORS 1w (5%) UNLESS OTHERWISE SPECIFIED;
ONE SIDE OF FILAMENT GROUNDED TO CHASSIS

Fig. 6.3. Servo for Curve Analyzer.

PHYSICS DIVISION QUARTERLY PROGRESS REPORT

part of a cycle. The fraction of a cycle over which they conduct depends on the magnitude of the input signal.

To prevent damage to the motor, the maximum voltage applied is limited by limiting the voltage applied to the grids of the thyratron by means of V-7. Variations in the load are compensated for by the back emf of the motor.

PRODUCTION AND DETECTION OF HEAVY IONS

G. E. Evans P. M. Stier
C. F. Barnette V. L. DiRito

During the past quarter the PIG-type ion source described in previous quarterly reports has been used for production of H^+ , He^+ , N^+ , N_2^+ , Ne^+ , A^+ , and A^{++} ions at energies of 50 to 300 keV. Analyzed beam currents of 100 to 150 μa normally have been used for the research described here, although several times this amount of current is available if needed. The particular source in use has been run satisfactorily for more than 500 hr

of operating time. A bench model of the source has been converted to include a resistance-heated source chamber to permit use of solid source materials.

The operation of a conventional electrostatic electron multiplier as a detector of low-energy heavy ions is being studied. In a preliminary experiment the counting efficiency of the electron multiplier for Po^{210} alpha particles has been measured roughly as 100%. Experimental equipment has been built that permits the exposure of the electron multiplier to a beam of ions of known intensity, energy, and mass. Ions are produced in a PIG-type source and are magnetically analyzed to select a desired energy and mass. A system of variable apertures permits extreme attenuation of the beam by known amounts so as to allow comparison of the electron multiplier output current (or counting rate) with the incident positive ion current as measured by an electrometer. N_2^+ ions of 10-keV energy have been detected with this apparatus in preliminary bench tests (see Fig. 6.4).

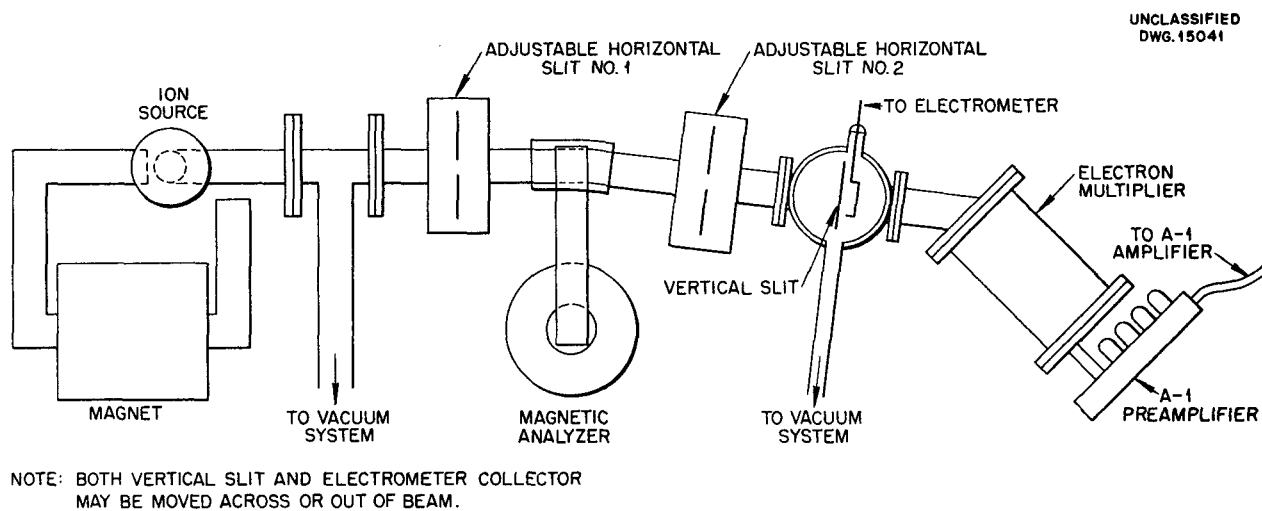


Fig. 6.4. Equipment for Ion Source and Electron Multiplier Response Studies.

OPTICS OF POLISHED SCINTILLATION
PHOSPHORS

UNCLASSIFIED
DWG. 15042

W. E. Millet⁽³⁾

Many factors are involved in obtaining good resolution with a scintillation spectrometer. One of the more important factors is the efficiency with which the light produced in the phosphor is collected onto the photocathode of the multiplier. The following analysis was undertaken in order to understand the nature of the collection process. Only polished surfaces were considered, although it has been observed experimentally that better resolution is obtained with ground surfaces.

A clear crystal in the form of a right-circular cylinder that has polished surfaces, with the top and bottom surfaces being plane and parallel to one another, will be considered (Fig. 6.5). If the index of refraction of the crystal is n_1 , if the top and side surfaces are in contact with air, and if the bottom surface is in optical contact with a clear medium that has an index of refraction, n_2 , where $n_1 > n_2 > 1$, the problem is to determine that fraction of the total light that leaves an isotropic point source within the crystal and enters into medium n_2 .

The first consideration will be the light from the point source that is directed into the lower hemisphere.

A ray incident upon the side of the crystal will be totally reflected if $\cos\theta > 1/n_1$, where θ is the angle between the ray and the axis of the crystal. This relation follows immediately from the condition for total internal reflection if the ray and the normal to the side at the point of reflection define a plane normal to the base. If this plane

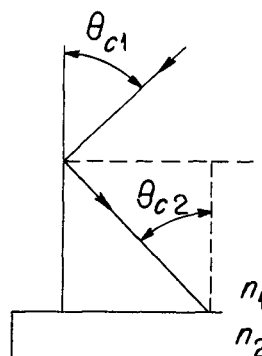


Fig. 6.5. Reflection of a Ray of Light from the Cylindrical Surface of a Polished Phosphor.

is other than normal to the base the inequality must still hold, since the angle of incidence is then still greater than the critical angle.

A ray striking the bottom of the crystal will be transmitted if $\sin\theta < n_2/n_1$. Let

$$\cos\theta_{c1} \equiv \frac{1}{n_1} \quad (1)$$

and

$$\sin\theta_{c2} \equiv \frac{n_2}{n_1} \quad (2)$$

If $\theta_{c1} = \theta_{c2}$, a ray that strikes the side at the critical angle will upon reflection strike the bottom at the critical angle. Then all light directed downward within a cone of half-angle θ_{c2} will enter medium n_2 whether or not the light in this cone strikes the side of the crystal first. Thus the fraction of the light directed in the lower hemisphere that enters medium n_2 is a constant independent of the position of the light source within the crystal. This is a very desirable situation from the standpoint of good resolution in gamma-ray scintillation spectrometers.

⁽³⁾University of Florida research participant.

PHYSICS DIVISION QUARTERLY PROGRESS REPORT

This situation will also be realized if

$$\theta_{c1} \geq \theta_{c2} . \quad (3)$$

If, however,

$$\theta_{c1} < \theta_{c2} , \quad (4)$$

the fraction of light entering medium n_2 is dependent upon the position of the light source within the crystal.

The light that goes into the upper hemisphere will now be considered (see Fig. 6.6). The light that will escape from the top must satisfy

$$\sin\theta < \frac{1}{n_1} .$$

If

$$\sin\theta_{ct} \equiv \frac{1}{n_1} ,$$

then

$$\theta_{ct} = \frac{\pi}{2} - \theta_{c1}$$

and

$$\theta_{ct} < \theta_{c2} .$$

UNCLASSIFIED
DWG. 15043

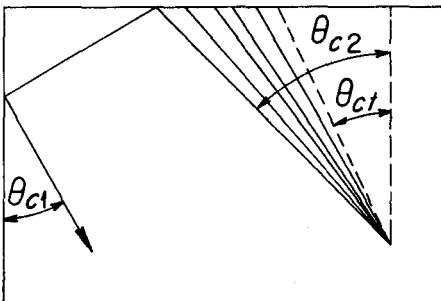


Fig. 6.6. Reflection of Light from the Top Surface of a Polished Phosphor.

Therefore, if $\theta_{c1} = \theta_{c2}$, that light going into the upward hemisphere, which lies between the cones having half-angles θ_{ct} and θ_{c2} , will be totally reflected. Here again it makes no difference if the light strikes the side before it strikes the top. If $\theta_{c1} > \theta_{c2}$, the previous analysis still applies. The case for $\theta_{c1} < \theta_{c2}$ is again undesirable and for the same reason as before.

The resolution of the gamma-ray spectrometer will be further improved if the total fraction of light entering n_2 is increased. Thus it would be desirable to reflect back to the crystal the light within the cone that has half-angle θ_{ct} .

It is seen from this analysis that for good resolution $\theta_{c1} \geq \theta_{c2}$, which may be rewritten in terms of the indices n_1 and n_2 :

$$\sin\theta_{c1} \geq \sin\theta_{c2} ,$$

$$\sqrt{1 - \cos^2\theta_{c1}} \geq \sin\theta_{c2} ,$$

$$\sqrt{1 - \left(\frac{1}{n_1}\right)^2} \geq \frac{n_2}{n_1} ,$$

or

$$n_2 \leq \sqrt{n_1^2 - 1} . \quad (3a)$$

The solid angle subtended by a cone of half-angle θ_{c2} is

$$\Omega = 2\pi (1 - \cos\theta_{c2}) .$$

By assuming that the reflector on the top surface is 100% effective, the

fraction of the total light that enters n_2 will be

$$f = \frac{2(2\pi)(1 - \cos\theta_{c2})}{4\pi}$$

$$= 1 - \cos\theta_{c2} = 1 - \sqrt{1 - \sin^2\theta_{c2}}$$

or

$$f = n_1 - \frac{\sqrt{n_1^2 - n_2^2}}{n_1}$$

Then by Eq. 3a,

$$f \leq \frac{n_1 - 1}{n_1}$$

The equality holds when $\theta_{c1} = \theta_{c2}$; i.e., when

$$n_2 = \sqrt{n_1^2 - 1}$$

It should be pointed out that if Eq. 3 is satisfied, the light that goes out the side of the crystal can never be reflected back into the crystal in such a manner as to make it pass into medium n_2 . This is true since the rays refracted out the side of the crystal have all angles represented, and any one of these when reflected back into the crystal must be within a cone of half-angle $(\pi/2 - \theta_{c1})$ and cone axis parallel to the base of the cylinder and will consequently not enter medium n_2 . It should also be noted that for a cylindrical crystal with a circular cross section, the amount of light escaping out the side of the crystal is not constant.

ADJUSTMENT OF
VOLTAGE DISTRIBUTION ON THE ELECTRODES
OF THE 5819 PHOTOMULTIPLIER

W. E. Millet

The photocurrent from different points on the photocathode was measured. A collection voltage of about 45 v between the photocathode and the multiplier unit was used while all of the multiplier dynodes were connected. An image of the face of a cathode-ray tube was focused on the photosurface of the 5819 photomultiplier. The beam of the cathode-ray tube was scanned along a straight line in the horizontal direction. The same scanning voltage was placed on the horizontal deflection plates of another cathode-ray tube, while the output of the phototube was amplified and fed onto the vertical deflection plates of the second cathode-ray tube. A plot of the sensitivity of the photosurface was then obtained along a line across the face of the phototube. This line could be moved to any line across the face of the tube, and plots obtained in this manner were painted on the face of the viewing cathode-ray tube. Reproduction of these plots for two different phototubes are given in Fig. 6.7. The deep dips in the response curves are caused by opaque patches placed on the face of the phototube for identification purposes.

After a series of these patterns had been outlined on the face of the viewing cathode-ray tube, the photomultiplier dynodes were connected with an appropriate voltage distribution. The voltage distribution on the dynodes that most nearly reproduced the photosensitivity patterns was then sought. No voltage distribution was found that

PHYSICS DIVISION QUARTERLY PROGRESS REPORT

UNCLASSIFIED
DWG. 15044

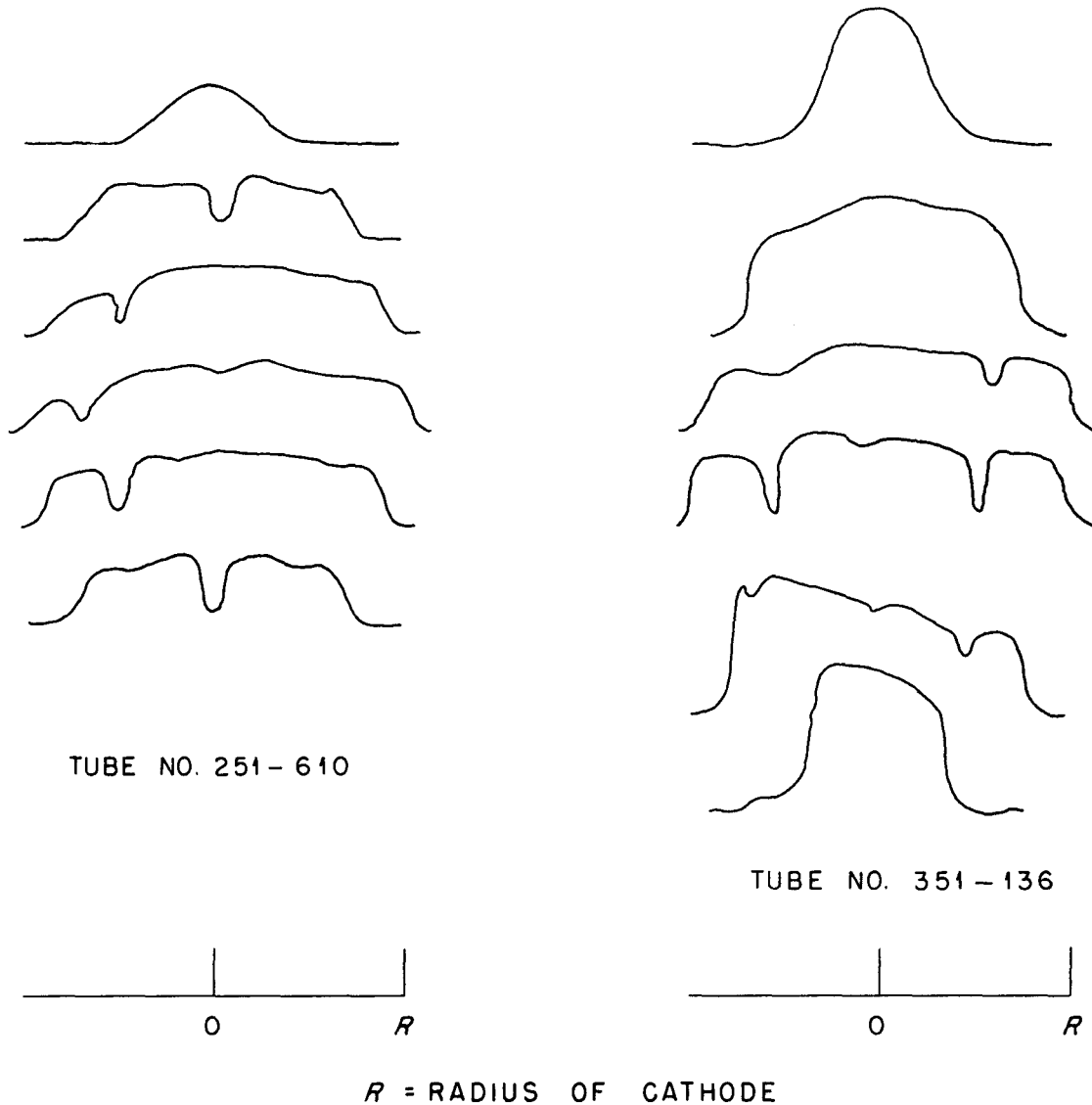


Fig. 6.7. Photocathode Emission Across the Cathode of Typical 5819 Photo-multipliers.

gave the same response as the photo-surface. A voltage distribution that gave a good reproduction of the photosensitivity curve along one line across the phototube gave a poor reproduction along another line. After this study was completed the tube was used in a scintillation spectrometer. It was

found that the resolution of the spectrometer was greatest for the voltage distribution that was found to reproduce most nearly the photosensitivity patterns.

Another experiment was carried out in an attempt to determine the best

voltage distribution on the dynodes. The dynode voltage distribution was set to that value which gave the best results in the previous experiment. The voltage between the photocathode and the first dynode was then varied, and the peak-to-valley ratio was measured. The over-all voltage on the voltage distribution was adjusted each time so that the photoelectric peak always occurred at the same pulse height. In some cases this meant that the gain of the amplifier had to be increased from 16 to as much as 64. The voltage distribution was indicated as follows:

$$(m, n, p, 1, 1, 1, 1, \dots),$$

where m is the ratio of the voltage difference between the photocathode and dynode 1 and the voltage difference between the last two dynodes, n is the ratio of the voltage difference between dynodes 1 and 2 and the voltage difference between the last two dynodes, etc.

Figure 6.8 shows three graphs of peak-to-valley ratio, one with m variable, one with n variable, and one with p variable.

EFFECT OF A LONGITUDINAL MAGNETIC FIELD ON THE RESOLUTION OF A 5819-NaI SCINTILLATION SPECTROMETER

W. E. Millet

In an effort to determine whether a magnetic field along the axis of the multiplier would improve the resolution of the scintillation spectrometer, the following experiments were conducted.

Helmholtz coils were mounted on the light shield. The strength and direction of the field were adjusted so that the horizontal component of the earth's field at the place at which the multiplier tube was to operate was cancelled. A magnetized needle floating

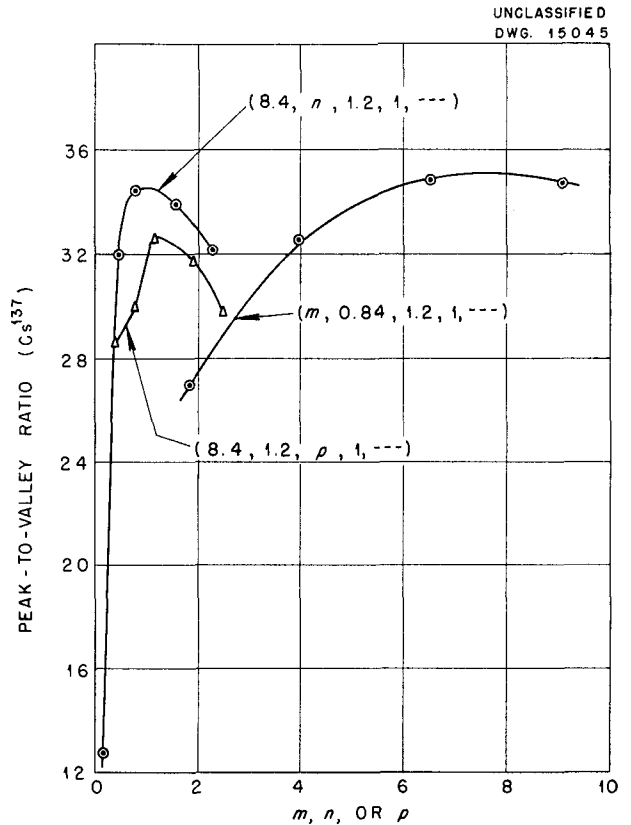


Fig. 6.8. Resolution of Scintillation Spectrometer as a Function of Collector Voltage and First and Second Dynode Voltages.

on water was used as an indicator for the field adjustment.

A solenoid with 120 turns was wound on a form about 2 in. in diameter and about 1 in. long. This coil was fitted over the 5819 multiplier that was mounted with the axis of the tube vertical. The coil then produced a field along the axis of the tube in the region between the photocathode and the multiplier unit.

There was an annoying decrease in the peak-to-valley ratio (Cs^{137}) during the course of the experiment. This may have been caused by a slight heating of the NaI crystal as a result of the current in the solenoid. The experiment was performed three times, and each

PHYSICS DIVISION QUARTERLY PROGRESS REPORT

time there was an indication that the peak-to-valley ratio was best for solenoid fields of zero and about 1.2 gauss upward, with a minimum at about 0.6 gauss upward. If the vertical component of the earth's field was 0.6 gauss downward, this would indicate that a field of about 0.6 gauss in either direction along the axis of the tube gave best results. The peak-to-valley ratio at ± 0.6 gauss was only 3 to 6% higher than it was at zero field ($P/v = 32$). At about 2 gauss downward the peak-to-valley ratio was down about 10%. This same behavior was noted in all three experiments, even though the order of taking the points on the curve was different in each case.

NEUTRON-SENSITIVE PHOSPHORS

J. Schenck

Crystals of LiI with thallium activation have been shown⁽⁴⁾ to respond to thermal neutrons.

In the course of testing the effect of various activators in LiI, it was found that a strong luminescence occurred under ultraviolet excitation when LiI was activated by tin. In order to determine its response to slow neutrons, crystals of this phosphor containing about 0.1 mole % of SnI_2 were grown from the melt. One of these crystals was selected that was about 1 by 0.5 by 0.5 cm, irregular in shape, transparent, and ranging in color from faint yellow to nearly colorless. The crystal was ground smooth on one side and optically connected to a 5819 photomultiplier through a lucite light piper (1 in. dia by 0.5 in. long). White vaseline was used to join the crystal, lucite, and photomultiplier. An aluminum can covering the crystal

and clamped with an "O" ring to the lucite served as a reflector and as a means of maintaining the crystal in an atmosphere of dry nitrogen.

The crystal was exposed to uncollimated neutrons from an unshielded polonium-beryllium source. A flux of slow neutrons was obtained by placing a block of paraffin behind the source. The measured photomultiplier pulse-height spectrum is shown in Fig. 6.9. Even in the presence of the gamma rays and fast neutrons emanating from the source, and in spite of the irregularity and nonuniformity of the crystal, the pulse-height spectrum exhibits a resolution of 15.1% for the monoenergetic excitation of the phosphor from the reaction of the moderated neutrons with the Li^6 .

Figure 6.10 shows the pulse-height spectrum of the same crystal and mounting with the peak caused by photoelectrons from Cs^{137} gamma radiation. A similar spectrum was taken

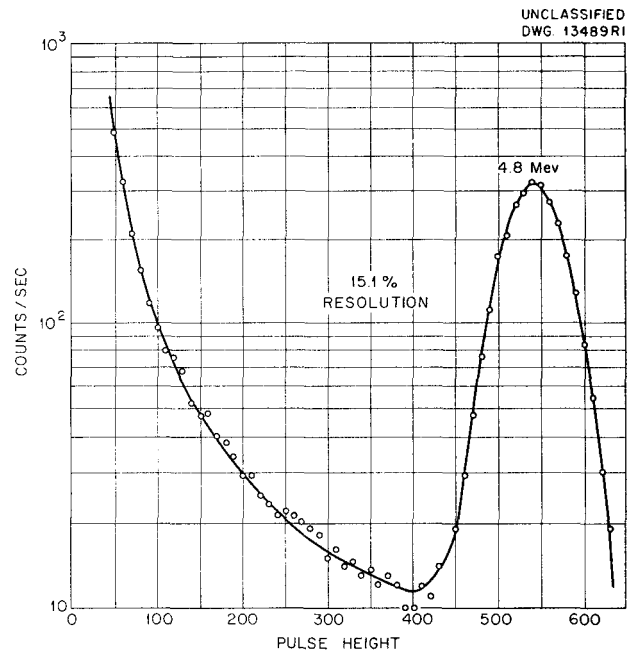


Fig. 6.9. Pulse Spectrum Produced in LiI (SnI_2 Activated) by Slow Neutrons.

⁽⁴⁾R. Hofstadter, J. A. McIntyre, H. Roderick, and H. I. West, Jr., "Detection of Slow Neutrons," *Phys. Rev.* **82**, 749 (1951).

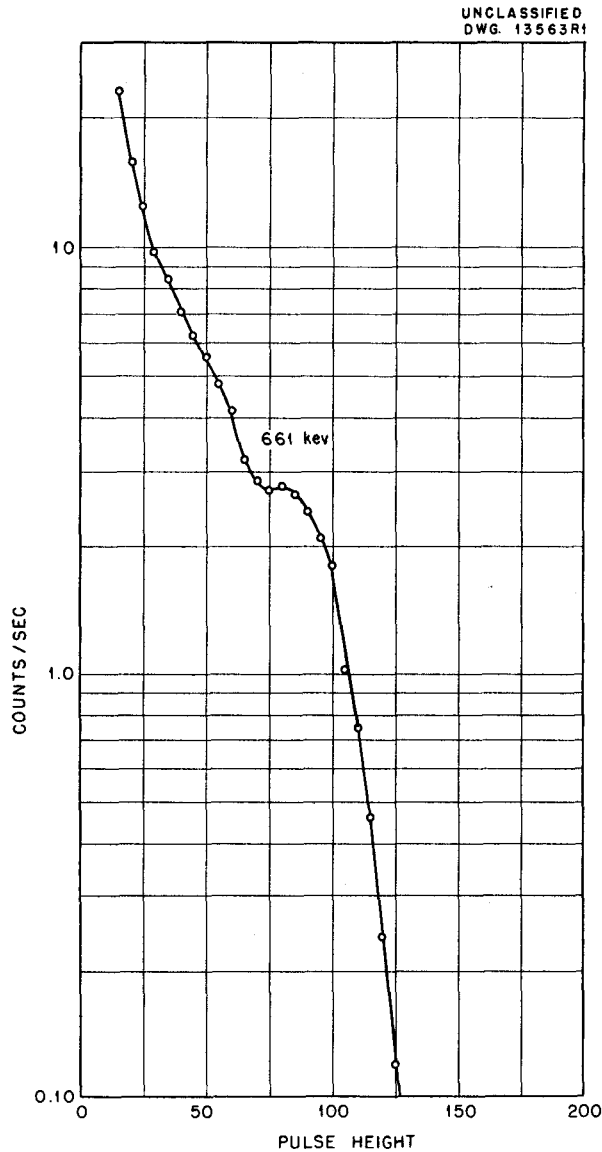


Fig. 6.10. Pulse Spectrum Produced in LiI (SnI₂ Activated) by Cs¹³⁷ Gamma Rays.

after replacing the LiI-SnI₂ with a NaI-TlI crystal. A comparison of the pulse heights at the photoelectric peaks gives an electron excitation efficiency for LiI-SnI₂ relative to NaI-TlI of 1/24.5. A comparison of the pulse heights with LiI-SnI₂ for Cs¹³⁷ gamma rays and for neutrons, assuming

linearity, gives a Q of 4.5 Mev for the $\text{Li}^6(n,\alpha)\text{H}^3$ reaction, which is 94% of the correct value of 4.785 Mev.

The scintillations produced by neutrons on LiI-SnI₂, which were detected by the photomultiplier, were observed on an oscilloscope, and the decay of fluorescence appeared to be purely exponential with a time constant of about 0.7 μsec .

In addition to the results obtained with LiI, it was found that tin will activate LiBr. A small amount of SnBr₂ was mixed with LiBr and melted in a pyrex test tube. After cooling, the white, microcrystalline mass gave a strong, white luminescence under ultraviolet excitation. When placed on the photomultiplier tube and exposed to thermal neutrons, the same sample produced large scintillation pulses that had a decay time constant of about 1.5 μsec . It is planned to grow single crystals of the bromide incorporating a number of different activators.

Investigation of oxygen-containing phosphors was continued, and many more samples, including silicates, titanates, phosphates, and stanates, were prepared and tested. The only good phosphor discovered was Li₂SnO₃ activated with 1 mole % TiO₂. The concentration of titanium could be varied over a range of ten to one without much change in the luminescence. The efficiency, emission spectrum, and decay time were found to be much the same as Ca₂WO₃. Instead of melting, Li₂SnO₃ decomposed when heated in a platinum crucible over a methane-oxygen flame.

The Li₂SnO₃ was prepared by a dry reaction of equimolar proportions of Li₂CO₃ and SnO₂ for several hours at a temperature of 1100°C in an air atmosphere. Since this compound was not found to be reported in the literature

and because there was a question about its existence, an x-ray diffraction pattern was taken of a powdered sample. The pattern gave evidence of a definite structure and showed only a small trace of unreacted SnO_2 and no lines corresponding to Li_2O or Li_2O_2 . The comparatively simple diffraction spectrum suggested the presence of a single phase.

**NEUTRON RESPONSE OF NaI
SCINTILLATION COUNTERS**

J. K. Bair H. B. Willard

In the attempt to measure the gamma-ray yield from the $\text{Li}^7(p,\gamma)\text{Be}^8$ reaction, it was discovered that the

NaI crystal scintillation counter does not have negligible sensitivity for low-energy neutrons (~ 30 to 100 kev). When biased to count all gamma pulses above 2 to 3 Mev, the yield curve followed very closely that of the $\text{Li}^7(p,n)\text{Be}^7$ reaction, exhibiting a geometric peak and the resonance at 2.25 Mev. The spectrum analysis indicates that this response is caused by gamma rays of ~ 8 Mev, presumably from neutron capture in the iodine. This capture cross section decreases with increasing neutron energy as was evidenced by the relative heights of the geometric peak and the 2.25-Mev resonance. For 30-kev neutrons, the efficiency for neutron capture seemed to be about 1% of that for gamma rays of equivalent energy.